AD_____

Award Number: DAMD17-98-1-8099

TITLE: Membrane-Bound Hyaluronidase in Breast Cancer Progression

PRINCIPAL INVESTIGATOR: Lurong Zhang, Ph.D.

CONTRACTING ORGANIZATION: Georgetown University
Washington, DC 20007

REPORT DATE: September 2001

TYPE OF REPORT: Annual

PREPARED FOR: U.S. Army Medical Research and Materiel Command
Fort Detrick, Maryland 21702-5012

DISTRIBUTION STATEMENT: Approved for Public Release;
Distribution Unlimited

The views, opinions and/or findings contained in this report are
those of the author(s) and should not be construed as an official
Department of the Army position, policy or decision unless so
designated by other documentation.

20020124 368

		Form Approved
REPORT DOCUMENTATION PAGE		OMB No. 074-0188

Public reporting burden for this collection of information is estimated to average 1 hour per response, including the time for reviewing instructions, searching existing data sources, gathering and maintaining the data needed, and completing and reviewing this collection of information. Send comments regarding this burden estimate or any other aspect of this collection of information, including suggestions for reducing this burden to Washington Headquarters Services, Directorate for Information Operations and Reports, 1215 Jefferson Davis Highway, Suite 1204, Arlington, VA 22202-4302, and to the Office of Management and Budget, Paperwork Reduction Project (0704-0188), Washington, DC 20503

1. AGENCY USE ONLY (Leave blank)	2. REPORT DATE September 2001	3. REPORT TYPE AND DATES COVERED Annual (1 Sep 00 - 31 Aug 01)	
4. TITLE AND SUBTITLE Membrane-Bound Hyaluronidase in Breast Cancer Progression			**5. FUNDING NUMBERS** DAMD17-98-1-8099
6. AUTHOR(S) Lurong Zhang, Ph.D.			

7. PERFORMING ORGANIZATION NAME(S) AND ADDRESS(ES) Georgetown University Washington, DC 20007 E-Mail: zhangl@georgetown.edu	8. PERFORMING ORGANIZATION REPORT NUMBER

9. SPONSORING / MONITORING AGENCY NAME(S) AND ADDRESS(ES) U.S. Army Medical Research and Materiel Command Fort Detrick, Maryland 21702-5012	10. SPONSORING / MONITORING AGENCY REPORT NUMBER

11. SUPPLEMENTARY NOTES
Report contains color

12a. DISTRIBUTION / AVAILABILITY STATEMENT Approved for Public Release; Distribution Unlimited	12b. DISTRIBUTION CODE

13. ABSTRACT (Maximum 200 Words)

Malignant tumor cells utilize the abnormally expressed enzymes to digest the surrounding matrix and make their way to invade and metastasize. We hypothesize that membrane-bound hyaluronidase (HAase, PH-20) may be one of these enzymes that can promote the tumor progression. In first two years, we have demonstrated: 1) HAase stimulated the colony formation via release the FGF-2 from immobilized form to free form, and then effective in a paracrine manner. This is also true using gene transfection approach; 2) transfection HAase cDNA into MDA231 breast cancer cells could enhance the tumor growth in CAM system; 3) HAase transfected MDA231 cells formed aggressive tumor via enhancement of angiogenesis. In past year, we focused on the expression of membrane-bound hyaluronidase in human breast cancer tissues. We had carefully designed the peptides that represented the antigenic domain of this enzyme and prepared the antibodies. The immunohistochemic staining was performed in 57 cases of human breast cancer tissues. The data indicated that the antibody could stain tumor cells with little background in the stroma. The positive staining rate was 83.3 % in metastatic breast cancer, while it was 55.5% in the non-metastatic tumors. Whether this enzyme can be a tumor marker will be further investigated.

14. SUBJECT TERMS Breast Cancer			15. NUMBER OF PAGES 34
			16. PRICE CODE

17. SECURITY CLASSIFICATION OF REPORT Unclassified	18. SECURITY CLASSIFICATION OF THIS PAGE Unclassified	19. SECURITY CLASSIFICATION OF ABSTRACT Unclassified	20. LIMITATION OF ABSTRACT Unlimited

NSN 7540-01-280-5500

Standard Form 298 (Rev. 2-89)
Prescribed by ANSI Std. Z39-18
298-102

Table of Contents

INTRODUCTION

The enzymes can digest the matrix surrounding tumor and enhance the tumor growth and metastasis by the following mechanism: **1)** to destroy the barrier that limits the space for tumor expanding; **2)** to release the growth factors that immobilized in the matrix, and to perform their stimulatory effects on tumor cells and endothelial cells in a paracrine manner; **3)** to invade into the vassals and allow the tumor cells to spread through blood/lymph paths (1-15).

Based on observations (16-36), we postulate that the membrane-bound hyaluronidase (HAase) that normally produced by only sperm is turn-on in undifferentiated breast cancer cells. This membrane-bound HAase might be utilized by tumor cells for the digest the existing HA and play a role in tumor progression.

To test our hypothesis, we proposed the following two aims:

(1) **The effects of human sperm-type membrane-bound hyaluronidase on tumor angiogenesis and metastasis.** The cDNA for sperm-type membrane-bound hyaluronidase will be subcloned into mammalian expression vector and transfected into breast cancer cells. The resulting cells will be examined: (a) *in vivo* tumor growth rate; (b) tumor metastases to lungs and lymph nodes; (c) tumor angiogenesis as judged by staining with anti CD-31. The results will be compared between transfectants receiving the hyaluronidase and those receiving the empty vector. If our hypothesis is correct, then the hyaluronidase transfected cells will be more aggressive with regard to growth rate, form more metastases and display a stronger degree of angiogenesis than the control cells.

(2) **Study of the expression of sperm-type membrane-bound hyaluronidase in primary and metastatic human breast cancer tissues.** Antibody against human sperm-type membrane-bound hyaluronidase will be generated by immunization of rabbits with synthetic peptides (20 mer) that were derived from different regions of the membrane-bound hyaluronidase. The resulting antibodies will be used in staining of breast cancer tissues. The expression levels of membrane-bound hyaluronidase will be compared between the primary tumors and metastatic tumors. If our hypothesis is correct, the hyaluronidase will be higher in some of the metastatic tumors than in the primary tumors. The correlation of expression levels of sperm-type membrane-bound hyaluronidase with tumor grade, metastasis and clinical outcome will be assessed to determine its possible diagnostic and prognostic value in human breast cancer.

This study will provide information concerning the role of membrane-bound hyaluronidase in the progression of human breast cancer and its possible diagnostic or prognostic value.

BODY

Aim 1. To test the hypothesis that over-expression of HAase increases the malignant potential of tumor cells.

In the passed two years, we have demonstrated: **1)** exogenous or genetically engineering expressed HAase could release FGF-2 from the immobilized form to the free form; **2)** the cells treated with exogenous HAase or transfected with cDNA of PH-20 had a higher levels of phosphorylation of tyrosine and MAPK compared to their counterparts; **3)** the cells treated with exogenous HAase or transfected with cDNA of PH-20 formed much bigger colonies colonies than the control; **4)** the conditional media from the PH-20 transfectants could stimulate the growth of endothelial cells in vitro; **5)** the PH-20 transfectants over-expressing HAase formed bigger tumors compared to the vector alone mock transfectants on tumor models in both CAM of chicken embryo and nude mice.

These data has been summarized as two abstracts and presented in 1999 and 2000 annual meeting of American Association for Cancer Research, and published in the Proceedings of American Association for Cancer Research.

Furthermore, we are submitting two papers to the peer-review journals and hopefully they will be published soon.

We feel that our funding is important to elucidate the role of HAase in tumor progression, especially we determine that the HAase can release the immobilized FGF2, which no one has reported before.

Aim 2. Study of the expression of sperm-type membrane-bound hyaluronidase in primary and metastatic human breast cancer tissues.

The purpose of this study is to see: 1) the incidence of membrane-bound HAase exists in human breast cancer; 2) the difference in the expression rate of HAase between the metastatic tumor and non-metastatic one, which will further confirm the role of HAase in tumor progression.

As planned in the proposal, in the third year, we were concentrated on the production of high quality anti-membrane-bound HAase. We also collected human breast tissue samples, optimize the conditions for the immunohistochemic staining, stained the samples and analyzed them. The results were reported as following:

1. Preparation of anti-HAase: For the determination of antigenic domain of PH-20, the GCG computer program was used to search the hydrophilic region and the surface region as well as other secondary structures of PH-20 HAase. The results (**Fig. 1**) indicated that the amino acid sequences 140 –200 was the mostly likelihood to sever as antigenic domains.
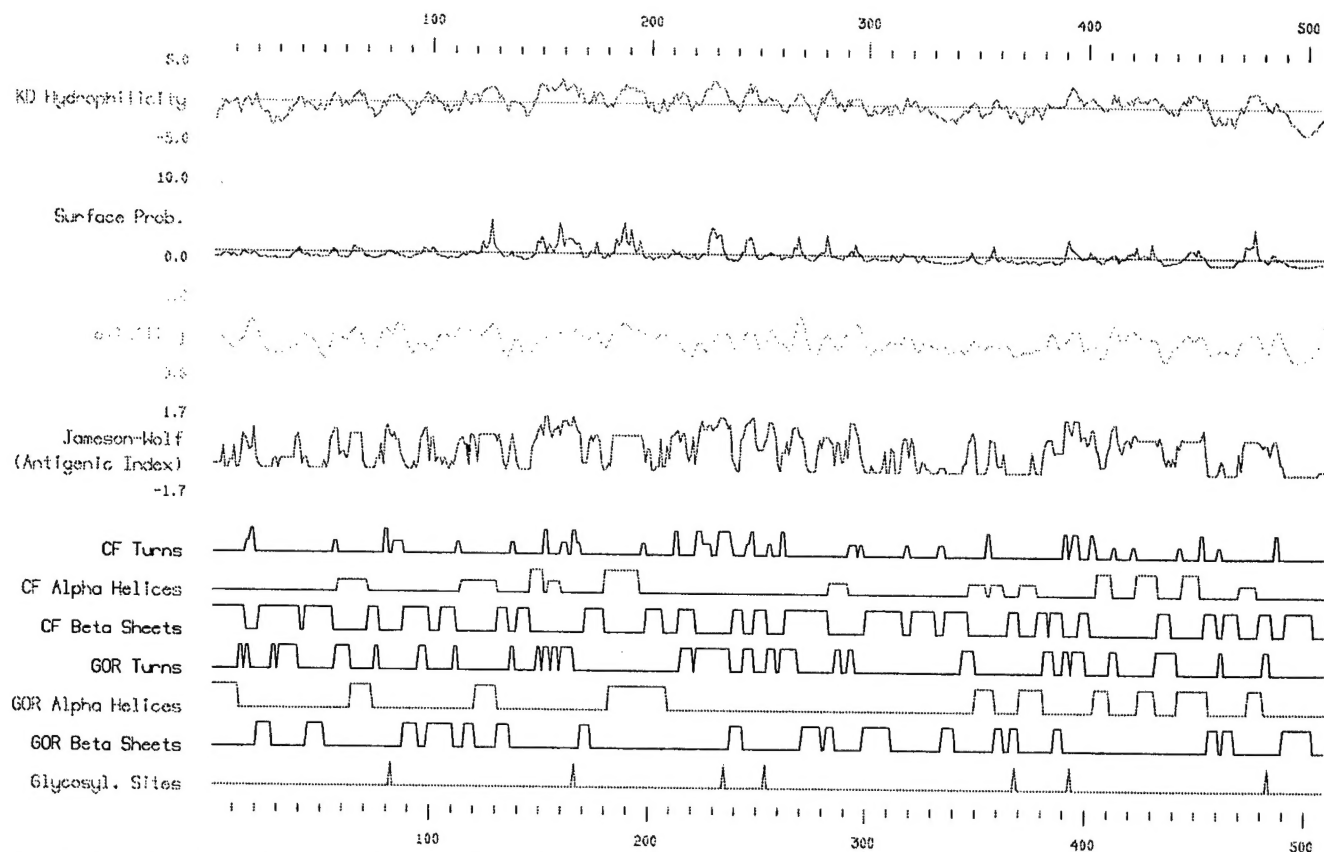
5

Figure 1. Determination of antigenic domains of PH-20. The profile of hydrophilic region, the surface region and other secondary structures of PH-20 were analyzed with GCG program and expressed as Plotstructure.

From 140 –200 region, we picked two sequences (**Fig. 2**) as antigens and commercially had them synthesized. Two synthetic peptides were conjugated with KLH to make the full-antigen.

```
  1  MGVLKFKHIF FRSFVKSSGV SQIVFTFLLI PCCLTLNFRA PPVIPNVPFL

 51  WAWNAPSEFC LGKFDEPLDM SLFSFIGSPR INATGQGVTI FYVDRLGYYP

                                                       148
101  YIDSITGVTV NGGIPQKISL QDHLDKAKKD ITFYMPVDNL GMAVIDWEEW

            167              180                          200
151  RPTWARNWKP KDVYKNRSIE LVQQQNVQLS LTEATEKAKQ EFEKAGKDFL

201  VETIKLGKLL RPNHLWGYYL FRDCYNHHYK KPGYNGSCFN VEIKRNDDLS

251  WLWNESTALY PSIYLNTQQS PVAATLYVRN RVREAIRVSK IPDAKSPLPV

301  FAYTRIVFTD QVLKFLSQDE LVYTFGETVA LGASGIVIWG TLSIMRSMKS

351  CLLLDNYMET ILNPYIINVT LAAKMCSQVL CQEQGVCIRK NWNSSDYLHL

401  NPDNFAIQLE KGGKFTVRGK PTLEDLEQFS EKFYCSCYST LSCKEKADVK

451  DTDAVDVCIA DGVCIDAFLK PPMETEEPQI FYNASPSTLS ATMFIVSILF

501  LIISSVASL*
```

Figure 2. The position and amino acid sequence of antigenic domains of PH-20. The amino acids (148 to 167 and 180 to 200) were chosen to synthesize as antigen according to the antigenicity analysis of GCG program.

6

In addition, the highly purified bovine sperm HAase was purchased from Sigma, which was used a native from of whole protein antigen. Six rabbits were immunized with these three antigens (two rabbits for each antigen) for three months. The serum was collected at different time points and the antibody titer was tested with ELISA. Briefly, the 96-well plate was coated with 10 µg/ml of HAase and blocked with 5% bovine albumin. The rabbit serum was serially diluted (from 1:1000 to 1:100,000) and added to the plate. After appropriate incubation and wash, the anti-rabbit secondary antibody conjugated with peroxidase was added followed by the substrate colorization. The results suggested that the titer of our anti-HAase were 1:10,000 to 1:100, 000.

When we directly used the antibody serum to stain the paraffin section, we found that the background of immunohistochemic staining was relatively high. To reduce the background, the antibody IgG portion from the rabbit serum was purified with protein G column. We also optimized the stain condition with the following approaches: 1) reiterative antigen of samples with microwave; 2) reduce the antibody concentration from 1:250 to 1: 1,000; and 3) intensively wash between each step. With these cares, the background staining was greatly reduced. While the tumor cells were strongly stained, the stromal was negative.

When the normal rabbit serum (prior to immunization) was used as first antibody instead of anti-PH 20 serum, there was no staining (**Fig 3** top panel) in a paired primary cancer (left) and lymph node metastases (right) collected from same patient, while there was a strong staining with anti-PH 20 (Fig 3 bottom panel). These data indicated that the antibody was specific.

Primary Breast Cancer   Lymph node metastasis(paired sample)

A

B

Staining with
normal serum
(prior to immunization)

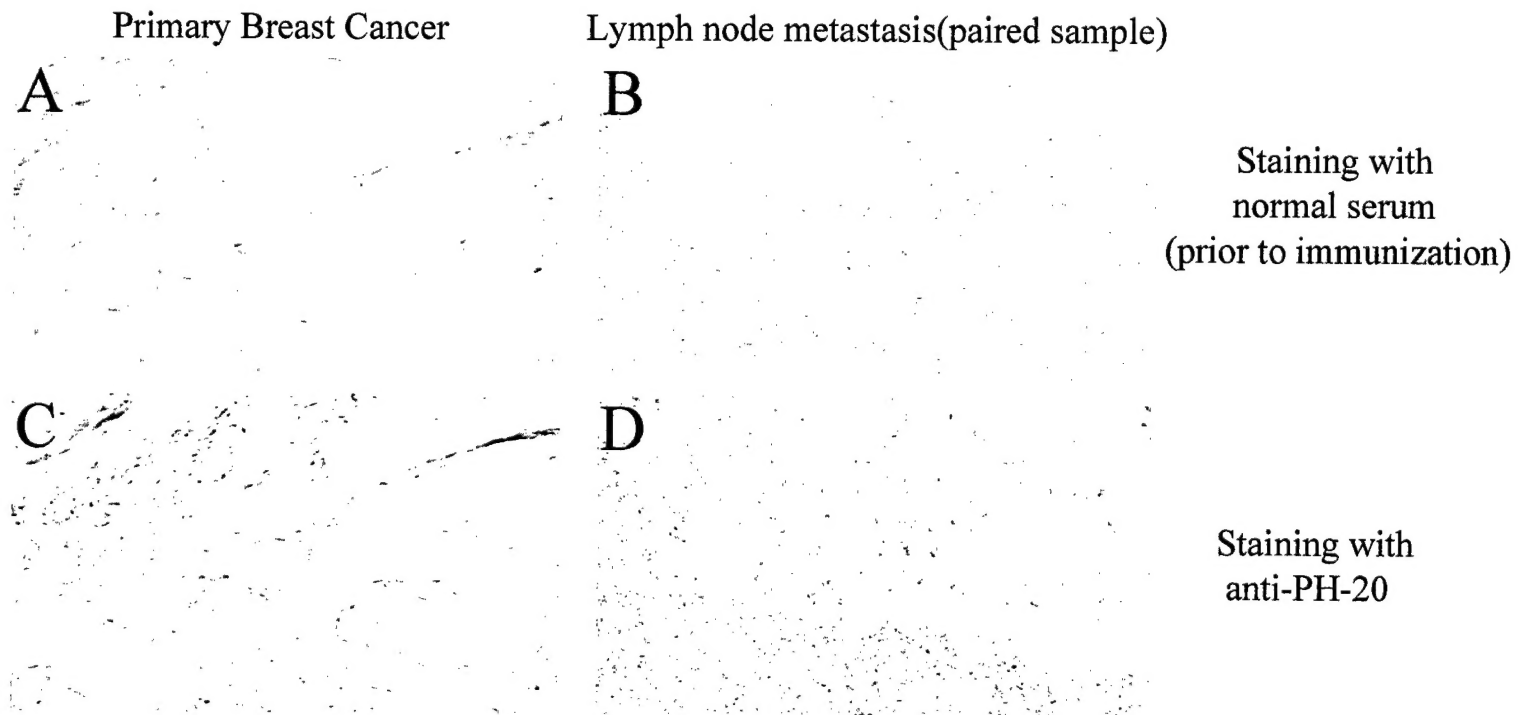**C**

D

Staining with
anti-PH-20

Figure 3. Determination of specificity of anti-PH-20 antibody. The serum collected from the rabbit prior to its immunization with HAase antigen or after immunization was used as primary reagent to stain a paired breast cancer sample. **Top panel**: staining with normal serum; **Bottom panel**: staining with anti- HAase; **Left side**: Primary cancer; **Right side**: Metastatic cancer in lymph node. There was no staining with normal serum (top panel), while a strong staining with anti-PH 20 was observed (bottom panel), indicating that the antibody was specific.

Then, the collected paraffin samples of human breast cancer were organized as groups: **1)** breast cancer without metastasis; **2)** primary breast cancer; **3)** lymph metastatic breast cancer. The group 2 and 3 were paired samples from the same patient, which was very valuable for the determination of the significance of sperm-type membrane-bound hyaluronidase in breast cancer progression.

First, the samples of breast cancer without metastasis were stained. While the background was relatively low, the cancer cells stained strongly with anti-HAase, indicating that breast cancer cells did express the PH-20 HAase (**Fig. 4**). In picture A and D of Fig. 4, the red positive staining was obviously surrounding the cancer cells, suggesting that it was the membrane-bound form. There were five cases stained positive and 4 cases negative. The positive rate was 55.5%.

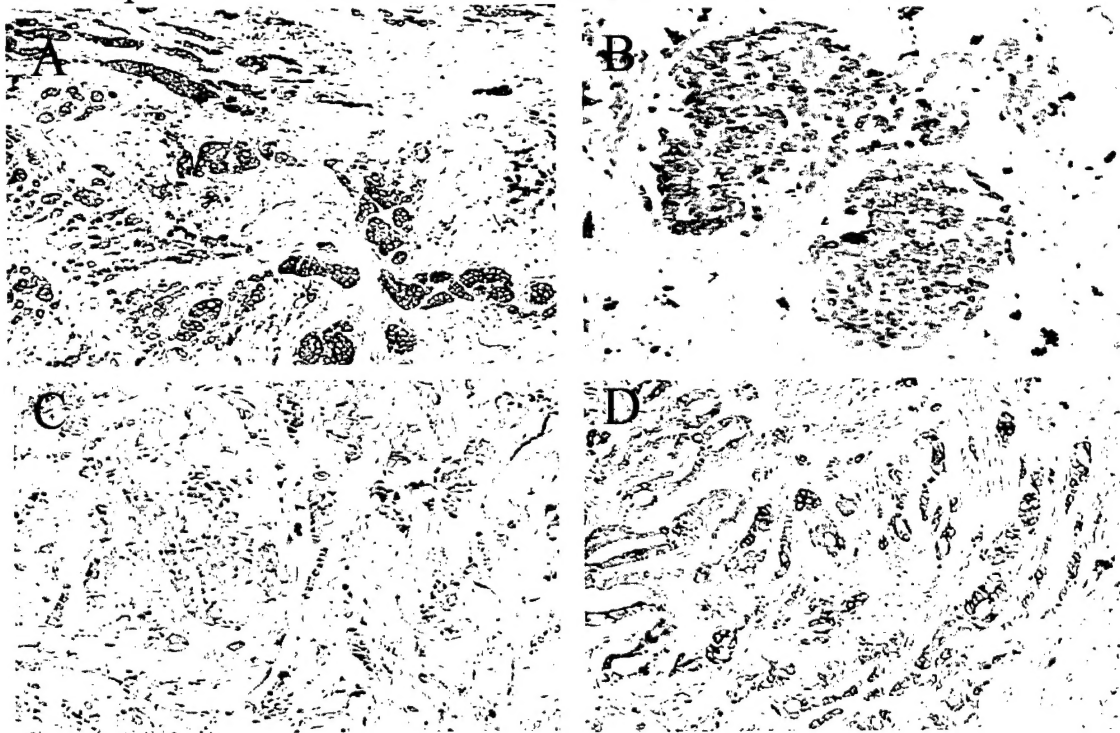Expression of HAase in Primary Breast Cancer Tissues

Figure 4. Expression of HAase in human primary breast cancer tissues. The five μm thick de-paraffin sections were stained with 1:500 diluted rabbit anti-PH-20 at 4°C overnight and then followed with ABC secondary staining kit (purchased from Bio-Media Inc. CA) and clorized with AEC in red. The cancer cells stained strongly with anti-PH-20 while little staining in surrounding stromal. A and D indicates that the staining is a membrane-bound type.

Secondly, the samples of metastatic breast cancer in lymph node were stained. The staining was also very intensive (**Fig 5**). There were 20 cases stained positive and 4 cases negative. The positive rate was 83.3%, which is much higher compared to the breast cancer without metastasis (83.3% v.s. 55.5%). This suggests that the cancer cells expressing PH-20 are likely to metastasize to remote organs and possess the expressing property in the new distant sites for the better settle-down and the growth into new tumors. The clear membrane staining pattern was also observed in D and E picture of figure 5. Again, this further confirmed the cellular location of this enzyme.

Expression of HAase in Breast Cancer
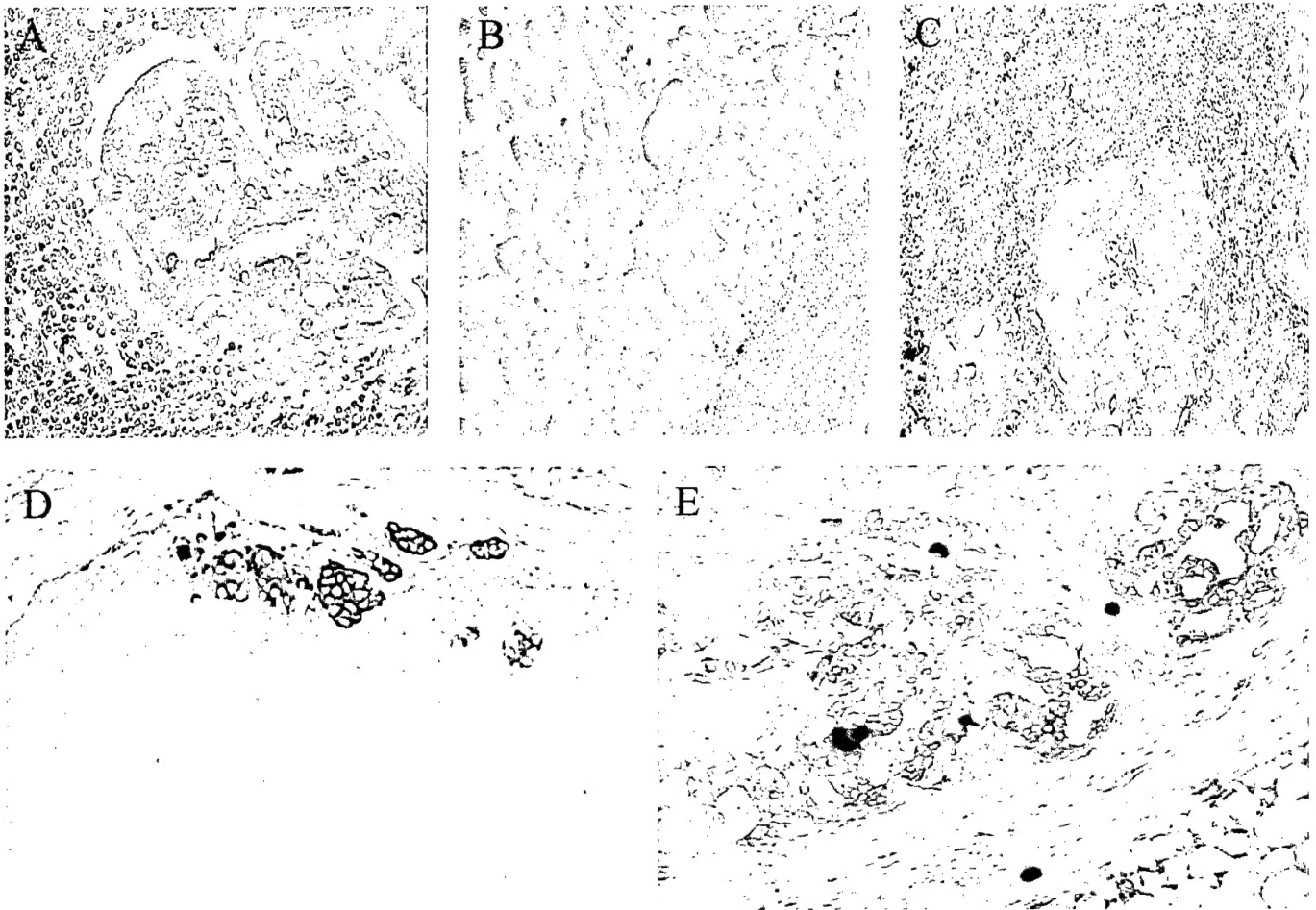# Lymph Node Metastases

Figure 5. Expression of HAase in human metastatic breast cancer in lymph node. The five μm thick de-paraffin sections were stained with 1:500 diluted rabbit anti-PH-20 at 4°C overnight and then followed with ABC secondary staining kit (purchased from Bio-Media Inc. CA) and clorized with AEC in red. While the staining of surrounding lymph tissue was negative, the metastatic cancer cells stained strongly with anti-PH-20. D and E indicated that the staining was surrounding the membrane. The positive rate was 83.3%, much higher than that in primary cancer without metastasis (55.5%).

It seems that metastatic cancer express PH-20 HAase in a much higher frequency than those primary cancers that had not metastasis when diagnosed and operated. To see if there is any difference in the expression level of PH-20 HAase between the cases with and without metastasis, the primary breast cancer samples from the patients with lymph node metastasis when diagnosed and operated were stained for HAase. Indeed, the results (**Fig 6** and **Table 1**) indicated that the HAase expression rate of breast cancer patients with metastasis was 70.8%, which was higher than that of patients without metastasis (70.8% v.s. 55.5%). This suggests that the cells expressing PH-20 HAase may have stronger ability to make their way to distant site via utilizing this matrix enzyme to destroy the integrity of surrounding tissue and vessels and to gain more support from released growth factors.

When we compared the HAase expression rate among 24 paired samples (primary and metastatic samples from the same patient), it was found that the expression rate in the metastatic samples was higher than

,that in their counterparts (83.3% v.s. 70.8%). This suggests that the metastasis process may preferentially select the cells that express high level of PH-20 HAase which would favor them to invade and colonize.

Expression of HAase in Paired
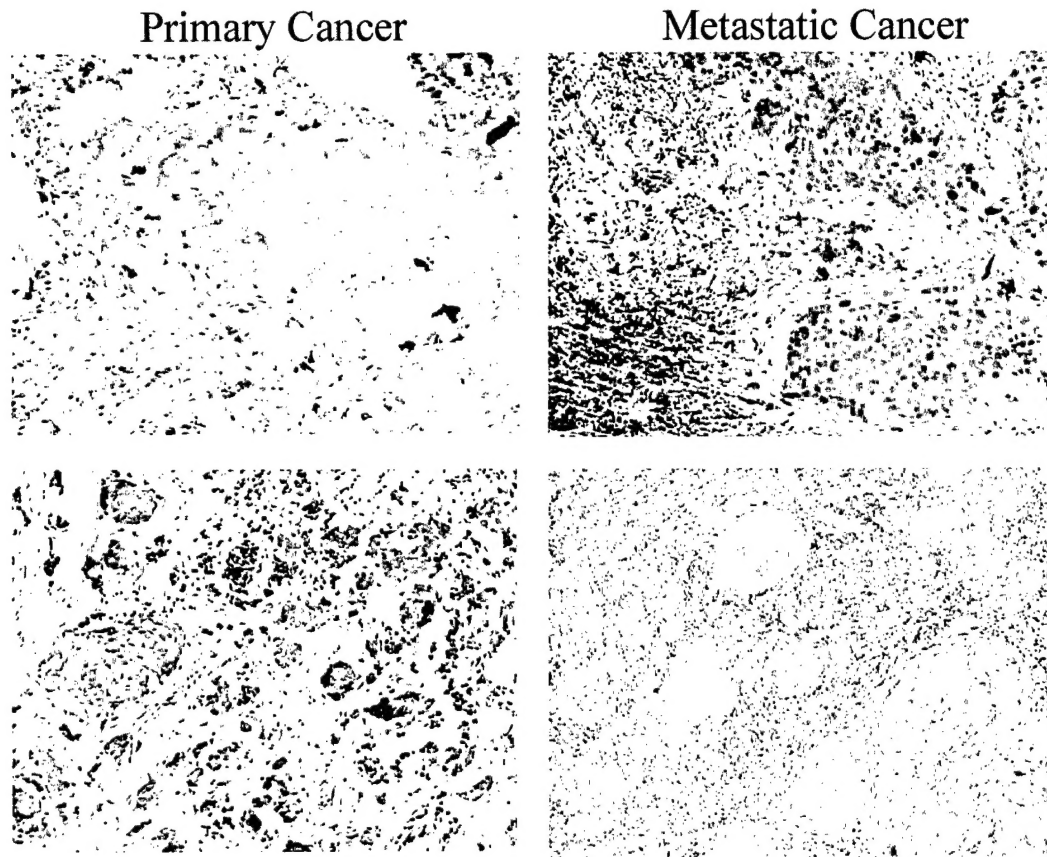## Primary and Metastatic Breast Cancer

Primary Cancer   Metastatic Cancer

Figure 6. Expression of HAase in primary and metastatic breast cancer. The paired samples of the primary and metastatic breast cancer were stained positively with anti-PH20. However, the positive staining rate in metastatic tumors was 83.3%, higher than that (70.8%) in primary tumors.

Table 1. Expression of HAase in Human Breast Cancer

Histopathology Type	Total Cases	Positive Cases	Nagetive Cases	Positive (%)
Breast Cancer with Lymph node metastasis	24	17	7	70.8
Metastasis Lymph Node Zone	24	20	4	83.3
Breast Cancer without Lymph nodes metastasis	9	5	4	55.5
Total	57	42	15	69.9

In summary, our results show that: **1)** PH-20 HAase in paraffin sections of human breast cancer can be stained with antibody generated with two peptides of PH-20 and bovine testes HAase from rabbit; **2)** the staining is in a peri-cellular pattern, indicating PH-20 HAase indeed is a membrane-bound enzyme; **3)** the positive staining rate in primary breast cancer without metastasis is 55.5%; in breast cancer with metastasis 70.8%; and in lymph node metastatic breast cancer 83.3%. These results suggest that PH-20 HAase is likely to play a role in breast cancer progression.

Although the data is encourage, to draw a defensive conclusion, we still need to do more experiments, such as staining more samples, including normal breast tissue and breast benign tumors. We also need to stain more cases for the statistic analysis. We will finish these works in the next year.

Key Research Accomplishments

- Generated anti-PH-20 HAase with two peptides of PH-20 and bovine testes HAase from rabbit, which is not commercially available.

- Purified IgG portions of the antibody and optimized its use condition for immunohistochemic staining. The material and the protocol may have commercial value.

- Collected valuable paired breast cancer samples (primary and metastatic samples from the same patient).

- Detected PH-20 HAase protein expressing in human breast cancer, which is not reported by other researcher yet.

- Stained certain amount of breast cancer samples and obtained some encourage results.

Reportable Outcomes

- **Publiscations (partially supported by this grant):**

1. Ningfei Liu, Charles B. Underhill, Randall Lapevich, Zeqiu Han, Feng Gao, Lurong Zhang and Shawn Green: Metastatin: A hyaluronan binding complex from cartilage inhibits tumor growth. Cancer Res. 2001; 61:1022-1028

2. Ningfei Liu, Feng Gao, Zeqiu Han, Charles B. Underhill and **Lurong Zhang:** Over-expression of Human Hyaluronan Synthase 3 in TSU Prostate Cancer Cells Promotes Tumor Growth. Cancer Res. 2001; 61: 5207-5214

- **Manuscripts:**

1. Lurong Zhang, Zeqiu Han, Ivan Ding, Ningfei Liu, Weiming Liu, Jianzhong Xie, Feng Gao and Charles B. Underhill: Hyaluronidase acts as a switch for fobroblast growth factor.

2. Feng Gao, Ningfei Liu, Zeqiu Han, Charles B. Underhill and Lurong Zhang: Over-expression of human membrane-bound hyaluronidase (PH-20) promotes tumor growth.

3. Luping Wang, Charles B. Underhill and Lurong Zhang: Expression of PH20 in human breast cancer

- **Abstract and presentation:**

1. Xue-Ming Xu, Yixin Chen[1], Ningfei Liu, Jinguo Chen, Feng Gao, Zequi Han, Charles B. Underhill and Lurong Zhang. Targeted peptide of human brain hyaluronan binding protein inhibits tumor growth. Proc. Annu. Meet. Am. Assoc. Cancer Res 2001; 42: 71:383

2. Feng Gao, Xue-Ming Xu, Charles B. Underhill, Shimin Zhang, Ningfei Liu, Zeqiu Han, Jiaying Zhang and Lurong Zhang. Human brain hyaluronan binding protein inhibits tumor growth via induction of apoptosis. Proc. Annu. Meet. Am. Assoc. Cancer Res 2001; 42: 815:4375

3. Ningfei Liu, Xue-Ming Xu, Charles B. Underhill, Susette Mueller, Karen Creswell, Yixin Chen, Jinguo Chen and Lurong Zhang. Inhibition of tumor growth by hyaluronan binding motifs (P4) is mediated by apoptosis pathway related with lysosome and mitochondria. Proc. Annu. Meet. Am. Assoc. Cancer Res 2001; 42: 644: 3465

4. Ningfei Liu, Xue-Ming Xu, Charles B. Underhill, Yixin Chen, Jinguo Chen, Feng Gao, Zeqiu Han and Lurong Zhang. Hyaluronan binding motifs inhibit tumor growth. Proc. Annu. Meet. Am. Assoc. Cancer Res 2001; 42: 71:382

5. Yixin Chen, Xue-Ming Xu, Jinguo Chen, Ningfei Liu, Charles B. Underhill, Karen Creswell, and Lurong Zhang. Anti-tumor effect of RGD-tachyplesin. Proc. Annu. Meet. Am. Assoc. Cancer Res 2001; 42: 69: 369

6. Jinguo Chen, Yixin Chen, Shuigen Hong, Fabio Leonessa, Robert Clake, Xue-Ming Xu, Ningfei Liu, Charles B. Underhill, Karen Creswell and Lurong Zhang. Effect of tachyplesin on MDR overexpressing tumor cells. Proc. Annu. Meet. Am. Assoc. Cancer Res 2001; 42: 812:4358

- **Antibody generated by supporting of this grant**

Rabbit antibodies against human membrane-bound HAase.

CONCLUSIONS

1. The rabbit antibodies against human membrane-bound HAase (PH-20) was successfully produced by Immunization with two peptides of PH-20 and bovine testes HAase.

2. The optimal condition for immunohistochemic staining (IHC) was established.

3. The results of IHC showed that the positive staining rate in primary breast cancer without metastasis is 55.5%; in breast cancer with metastasis 70.8%; and in lymph node metastatic breast cancer 83.3%. These results suggest that PH-20 HAase is likely to play a role in breast cancer progression.

References

1. Brown JM; Giaccia AJ: The unique physiology of solid tumors: opportunities (and problems) for cancer therapy. Cancer Res 1998; 58(7):1408-16

2. Russell PJ; Stricker P; Bennett S: Growth factor involvement in progression of prostate cancer. Clin Chem 1998;44(4):705-23

3. Levine MD; Stracke ML; Liotta LA: Stimulation and regulation of tumor cell motility in invasion and metastasis. EXS 1995;74:157-79

4. Griffiths L; Stratford IJ: Platelet-derived endothelial cell growth factor thymidine phosphorylase in tumourgrowth and response to therapy. Br J Cancer 1997;76(6):689-93.

5. Nguyen M: Angiogenic factors as tumor markers. Invest New Drugs 1997;15(1):29-37

6. Walker RA; Shaw JA; Walsh T; Chappell S; Jones JL: Molecular pathology of breast cancer and its application to clinical management. Cancer Metastasis Rev 1997 16(1-2):5-27

7. Dimitriadou V; Koutsilieris M: Mast cell-tumor cell interactions: for or against tumour growth and metastasis? Anticancer Res 1997;17(3A):1541-9

8. Wright JA; Huang A: Growth factors in mechanisms of malignancy: roles for TGF-beta and FGF. Histol Histopathol 1996; 11(2):521-36

9. Folkman, J. and Shin, Y. : Angiogenesis. J. Biol. Chem. 1992; 267: 10931-10934.

10. Plate, K. H., Breier, G., Weich, H. A., and Risau, W. : Vassel endothelial growth factor is a potential tumor angiogenesis factor of human gliomas in vivo. Nature (Lond.) 1992; 359: 845-847.

11. Kim, K. J., Li. B., Winer, J., Armanini, M., and Gillet, N.: Inhibition of vascular endothelial-growth-factor-induced angiogenesis suppresses tumor growth in vivo. Nature (Lond.) 1993; 362: 841-844.

12. Ishikawa, F., Miyazono, K., Hellman, U., Drexler, H., Wernstedt, C., Hagiwara, K., Usuki, K., Takaku, F., Risau, W., and Heldin, C. H.: Identification of angiogenic activity and the cloning and expression of platlet-derived endothelial-cell growth factor. Nature (Lond.) 1989; 338: 557-562.

13. Nabal, E. G., Yang, Z., Plants, G., Forough, R., Zhang, S., Haudenschild, C.C. Macaig, T. and Nabel, G. J.: Recombinant fibroblast growth factor-1 promotees intimal hyperplasia and angiogenesis in arteries in vivo. Nature (Lond.) 1993; 362: 844-846.

14. Schreiber, A. B., Winkler, M. E., and Derynck, R.: Trqansforming growth factor alpha: a more potent angiogenesis mediatro than epidermal growth factor. Science 1986; 232: 1250-1253.

15. Frater-Schroeder, M. F., Risau, W., Hallmann, R., Gautschi, P. and Bohlen, P.: Tumor necrosis factor type-alpha, a potent inhibitor of endothelial -cell growth in vitro, is angiogenic in vivo. Proc. Nat. Acad. Sci. (Wash) 1987;84: 5277-5281.

16. Zhang L; Kharbanda S; Chen D; Bullocks J; Miller DL; Ding IY; Hanfelt J; McLeskey SW; Kern FG: MCF-7 breast carcinoma cells overexpressing FGF-1 form vascularized, metastatic tumors in ovariectomized or tamoxifen-treated nude mice. Oncogene 1997; 15(17):2093-108

17. Czubarko, F., Liaudet-Coopman, E. D. E., Aigner, A., Tuveson, A.T., Berchem, GJ and Wellstein, A: A secreted FGF-binding protein can serve as the angiogenic switch in human cancer. Nature Medicine 1997; 3 (10): 1137-1140

18. Pham, H. T., Block, N. L., Lokeshwar, V. B.: Tumor-derived hyaluronidase: A diagnostic urine marker for high-grade bladder cancer. Cancer Res. 1997; 57: 778-783

19. Lokeshwar VB, Lokeshwar BL, Pham HT, Block NL: Association of elevated levels of hyaluronidase, a matrix-degrading enzyme, with prostate cancer progression. Cancer Res 1996; 56(3):651-7

20. Cameron, E.: Hyaluronidase and Cancer. Pergamon Press 1966

21. Lin, R.Y., Argenta, P. A., Sullivan, K. M. Stern, R., and Adzick, N. S.: Urinary hyaluronic acid is a Wilms' tumor marker. J. Pedistr. Surg. 1995; 30: 304-308

22. Bok SW : Hyaluronidase, from wound healing to cancer (II). Med Hypotheses 1982; 8(5):455-9

23. Stern, M., Longaker, M. T., Adzick, N. S., Harrison, M. R., and stern, R.: Hyaluronidase levels in urine from Wilms' tumor patients J. Natl. Cancer. Inst. 1991; 83: 1569-1574

24. Lin, R.Y., Argenta, P. A., Sullivan, K. M. Stern, R., and Adzick, N. S.: Urinary hyaluronic acid is a Wilms' tumor marker. J. Pedistr. Surg. 1995; 30: 304-308

25. Pham, H. T., Block, N. L., Lokeshwar, V. B.: Tumor-derived hyaluronidase: A diagnostic urine marker for high-grade bladder cancer. Cancer Res. 1997; 57: 778-783

26. Liu D; Pearlman E; Diaconu E; Guo K; Mori H; Haqqi T; Markowitz S; Willson J; Sy MS: Expression of hyaluronidase by tumor cells induces angiogenesis in vivo. Proc Natl Acad Sci U S A 1996 Jul 23; 3(15):7832-7

27. Hakanson, E. Y. and Glick, D.: J. Nat. Cancer Inst. 1948; 9: 129

28. Gmachl, M., Sagan, S.. Ketter, S and Kreil, G.: The human sperm protein PH-20 has hyaluronidase activity. FEBS 1993; 336 (3): 545-548.

29. Lin, Y., Kimmel,L. H., Myles, D. G., and Primakoff, P.: Molecular cloning of the human and monkey sperm surface protein PH-20. Proc. Natl. Acad. Sci. USA 1993; 90: 10071-10075.

30. Primakoff, P., Hyatt, H. and Myles, D. G. J. Cell Biol. 1985; 101: 2239-2244.

31. West, D.C., Hampson, I. N., Arnold, F. and Kumar, S.: Angiogenesis induced by degradation products of hyaluronic acid. Science 1985; 228: 1324-1326.

32. Zhang L; Kharbanda S; Hanfelt J; Kern FG: Both autocrine and paracrine effects of transfected acidic fibroblast growwth factor are involved in the estrogen-independent and antiestrogen-resistant growth of MCF-7 breast cancer cells. Cancer Res 1998; 8 (2): 352-61.

33. Engelberg, H.: Action of heparin that may affect the malignant process. Cancer 85 (2): 257-272; 1999

34. Eccles, S. A.: Heparanse: Breasking down barriers in tumors. Nat. Med. 5 (7): 735-736; 1999

35. Rak, J and Kerbel, R. S.: b-FGF and tumor angiogenesis—Back in the limelight. Nat. Med. 3 (10): 1083-1084; 1997

36. Czubayko, F., Smith, R.V., Chung, H. C., and Wellstein, A. Tumor growth and angiogenesis induced by a secreted binding protein for fibroblast growth factors. J. Biol. Chem. 269: 28243-28248, 1994

Appendices

- ## Publiscations (partially supported by this grant):

1. Ningfei Liu, Charles B. Underhill, Randall Lapevich, Zeqiu Han, Feng Gao, Lurong Zhang and Shawn Green: Metastatin: A hyaluronan binding complex from cartilage inhibits tumor growth. Cancer Res. 2001; 61:1022-1028

2. Ningfei Liu, Feng Gao, Zeqiu Han, Charles B. Underhill and Lurong Zhang: Over-expression of Human Hyaluronan Synthase 3 in TSU Prostate Cancer Cells Promotes Tumor Growth. Cancer Res. 2001; 61: 5207-5214

- ## Abstract and presentation:

1. Xue-Ming Xu, Yixin Chen[1], Ningfei Liu, Jinguo Chen, Feng Gao, Zequi Han, Charles B. Underhill and Lurong Zhang. Targeted peptide of human brain hyaluronan binding protein inhibits tumor growth. Proc. Annu. Meet. Am. Assoc. Cancer Res 2001; 42: 71:383

2. Feng Gao, Xue-Ming Xu, Charles B. Underhill, Shimin Zhang, Ningfei Liu, Zeqiu Han, Jiaying Zhang and Lurong Zhang. Human brain hyaluronan binding protein inhibits tumor growth via induction of apoptosis. Proc. Annu. Meet. Am. Assoc. Cancer Res 2001; 42: 815:4375

3. Ningfei Liu, Xue-Ming Xu, Charles B. Underhill, Susette Mueller, Karen Creswell, Yixin Chen, Jinguo Chen and Lurong Zhang. Inhibition of tumor growth by hyaluronan binding motifs (P4) is mediated by apoptosis pathway related with lysosome and mitochondria. Proc. Annu. Meet. Am. Assoc. Cancer Res 2001; 42: 644: 3465

4. Ningfei Liu, Xue-Ming Xu, Charles B. Underhill, Yixin Chen, Jinguo Chen, Feng Gao, Zeqiu Han and Lurong Zhang. Hyaluronan binding motifs inhibit tumor growth. Proc. Annu. Meet. Am. Assoc. Cancer Res 2001; 42: 71:382

5. Yixin Chen, Xue-Ming Xu, Jinguo Chen, Ningfei Liu, Charles B. Underhill, Karen Creswell, and Lurong Zhang. Anti-tumor effect of RGD-tachyplesin. Proc. Annu. Meet. Am. Assoc. Cancer Res 2001; 42: 69: 369

6. Jinguo Chen, Yixin Chen, Shuigen Hong, Fabio Leonessa, Robert Clake, Xue-Ming Xu, Ningfei Liu, Charles B. Underhill, Karen Creswell and Lurong Zhang. Effect of tachyplesin on MDR overexpressing tumor cells. Proc. Annu. Meet. Am. Assoc. Cancer Res 2001; 42: 812:4358

Hyaluronan Synthase 3 Overexpression Promotes the Growth of TSU Prostate Cancer Cells[1]

Ningfei Liu, Feng Gao, Zeqiu Han, Xueming Xu, Charles B. Underhill, and Lurong Zhang[2]

Department of Oncology, Lombardi Cancer Center, Georgetown University Medical School, Washington DC 20007

ABSTRACT

Hyaluronan synthase 3 (HAS3) is responsible for the production of both secreted and cell-associated forms of hyaluronan and is the most active of the three isoforms of this enzyme in adults. In this study, the cDNA for human HAS3 was cloned and characterized. The open reading frame consisted of 1659 bp coding for 553 amino acids with a deduced molecular weight of about 63,000 and isoelectric pH of 8.70. The sequence of human HAS3 displayed a 53% identity to HAS1 and a 67% identity to HAS2. It also contained a signal peptide and six potential transmembrane domains, suggesting that it was associated with the plasma membrane. To evaluate the physiological role of human HAS3, expression vectors for this protein were transfected into TSU cells (a prostate cancer cell line), and the phenotypic changes in these cells were examined. The enhanced expression of hyaluronan in the transfected cells was demonstrated by dot blot analysis and ELISA. These cells were found to differ from their vector-transfected counterparts with respect to the following: (*a*) they grew at a faster rate in high (but not low) density cultures; (*b*) conditioned media from these cells stimulated the proliferation and migration of endothelial cells; (*c*) when placed on the chorioallantoic membrane of chicken embryos, these cells formed large, dispersed xenografts, whereas the control transfectants formed compact masses; and (*d*) when injected s.c. into nude mice, the xenografts formed by HAS3 transfectants were bigger than those formed by control transfectants. Histological examination of these xenografts revealed the presence of extracellular hyaluronan that could act as conduits for the diffusion of nutrients. In addition, they had a greater number of blood vessels. However, the HAS3-transfected TSU cells did not display increased metastatic properties as judged by their ability to form lung masses after i.v. injection. These results suggested that the HAS3-induced overexpression of hyaluronan enhanced tumor cell growth, extracellular matrix deposition, and angiogenesis but was not sufficient to induce metastatic behavior in TSU cells.

INTRODUCTION

A number of studies have suggested that the production of hyaluronan is associated with the metastatic behavior of tumor cells (1–11); *e.g.*, Toole *et al.* (1) have shown that invasive tumors formed by V2 carcinoma cells in rabbits have higher concentrations of hyaluronan than noninvasive tumors formed by these same cells in nude mice. Similarly, Kimata *et al.* (2) found that a strain of mouse mammary carcinoma cells with a high metastatic potential produced significantly greater amounts of hyaluronan than a similar strain with a low metastatic potential. In a previous study (3), we found that the amount of hyaluronan on the surfaces of mouse B16 melanoma cells was directly correlated with their ability to form lung metastases. Finally, increased levels of hyaluronan production have been correlated with a variety of metastatic tumors, including carcinomas of the breast, lung,

liver, pancreas, and kidney (Wilms' tumor) (4–9). Indeed, in the case of Wilms' tumor (10) and mesotheliomas (11), the increased levels of hyaluronan in the serum of these patients has been regarded as a diagnostic marker for the clinical course of these conditions. Thus, there appears to be a correlation between hyaluronan production and metastatic behavior.

At present, three closely related isoforms for HAS[3] have been described, termed HAS1, 2, and 3, each of which appears to be associated with the plasma membrane (12–19). They have a predicted molecular mass of approximately 63 kDa, and transfection of cells with expression vectors for each of these isoforms can induce the synthesis of hyaluronan and the formation of a pericellular coat. However, the three isoforms are distinguished from each other with respect to: (*a*) their expression pattern during embryonic development and distribution in adult tissues; (*b*) the phenotype of knockout mutants in mice in which loss of HAS2 resulted in an embryonic lethality, whereas ones deficient in HAS1 and HAS3 were viable and had no obvious phenotype; (*c*) the rate at which they carry out hyaluronan synthesis, with HAS3 being more active than either HAS1 and HAS2; and (*d*) the size of the hyaluronan produced by the different isoforms with HAS3 giving rise to a somewhat smaller product than either HAS1 or 2 (17, 18).

Several recent studies have shown that transfection of tumor cells with expression vectors for hyaluronan synthase alters their behavior; *e.g.*, Kosaki *et al.* (20) reported that the transfection of human fibrosarcoma cells with HAS2 enhanced both anchorage-independent growth and tumorigenicity. In addition, Itano *et al.* (21) have found that clones of mouse mammary cancer cells that had low levels of hyaluronan synthesis demonstrated decreased metastatic properties, which could be restored if the cells were transfected with an expression vector for HAS1.

In this study, we have cloned and characterized the full-length cDNA for human HAS3 and examined its potential role in tumor progression. An expression vector carrying HAS3 was transfected into TSU prostate cancer cells, and alterations in the phenotype of the resulting cells were examined. We found that the HAS3-induced overexpression of hyaluronan enhanced the rate of tumor cell growth both *in vitro* and *in vivo*. Xenografts of the HAS3-transfected cells grew faster and larger, demonstrated a hyaluronan-rich stroma and increased vascularization. However, transfection with HAS3 did not shift the TSU cells to a more metastatic phenotype, suggesting that hyaluronan alone is not sufficient for metastasis in the case of TSU cells.

MATERIALS AND METHODS

Cell Lines. The TSU human prostate cancer cell line was obtained from the Tumor Cell Line Bank of the Lombardi Cancer Center (Georgetown University, Washington DC) and maintained in 10% calf serum, 90% DMEM. ABAE cells were kindly provided by Dr. Luyuan Li (Lombardi Cancer Center, Washington DC) and were cultured in 10% fetal bovine serum, 90% DMEM containing 2 ng/ml basic fibroblast growth factor.

[3] The abbreviations used are: HAS, hyaluronan synthase; ABAE, adult bovine aorta endothelial cells; b-HABP, biotinylated hyaluronan-binding protein from cartilage; RT-PCR, reverse transcription-polymerase chain reaction.

Cloning and Characterization of cDNA for Human HAS3. Oligonucleotide primers for PCR of a partial sequence of cDNA for human HAS3 were designed according to the published sequence of Spicer and McDonald (Ref. 17; GenBank accession no. U86409) and consisted of the following: 5'-TCCTACTTTGGCTGTGTGCAG and 3'-AGATTTGTTGATGGTAGCAAT. A human brain cDNA library (Clontech, Palo Alto, CA) was used as a template, and PCR was performed to generate a 570-bp fragment of human HAS3 cDNA. This fragment was then used to probe the human brain cDNA library. Positive clones were isolated, amplified, and sequenced. The MacVector program was used to carry out homologue analysis of the cloned human HAS3 with other human and mouse HASs.

Construction and Transfection of Human HAS3 Expression Vector. The cDNA for HAS3 was subcloned into the pcDNA3 mammalian expression vector (Invitrogen, Carlsbad, CA), and correct clones were identified by restriction endonuclease map analysis. The HAS3-pcDNA3 or pcDNA3 (control vector) were transfected into TSU cells using the calcium precipitation method (22). The clones that survived in 1 mg/ml of Geneticin (G418) (>100 individual clones in each case) were pooled and expanded further for characterization.

Characterization of Transfected Cells. The presence of HAS3 message was determined by RT-PCR using the GeneAmp RNA PCR kit (Perkin-Elmer, Branchburg, NJ). The primers consisted of the following: 5'-TCATGGTGGT-GGATGGCAACCGC and 3'-CTAAGCCACCTGATGTACGTCCA, which gave rise to a 283-bp reaction product with HAS3 and a 324-bp product with HAS1. The amplified sequences were analyzed by agarose gel electrophoresis followed by staining with ethidium bromide.

Two methods were used to determine hyaluronan production by the transfected cells. The first consisted of dot blot analysis of secreted hyaluronan, in which conditioned media from vector-TSU and HAS3-TSU cells that had been cultured at similar densities for 3 days were applied to nitrocellulose membrane using a dot blot apparatus. After washing with PBS containing 0.1% Tween 20, the membrane was blocked with 5% nonfat milk and 1% polyvinylpyrrolidone in PBS for 30 min. The hyaluronan was detected by sequential incubations in 1 μg/ml of b-HABP (23) for 1 h, 0.25 μg/ml of peroxidase-labeled streptavidin for 1 h, and finally a chemiluminescent substrate for peroxidase.

The second method for quantitation of hyaluronan consisted of a modified enzyme-linked assay (23). For this assay, a high-bound ELISA plate (Falcon, Lincoln Park, NJ) was coated with 100 μg/ml of crude human umbilical cord hyaluronan (Sigma Chemical Co., St. Louis, MO) in PBS at room temperature overnight and blocked with 10% calf serum, 90% PBS. The samples of conditioned media and cell lysates were adjusted to equal protein concentrations, and 25-μl samples were mixed with 100 μl of 50 μg/ml of b-HABP at 37°C for 1 h and then transferred to the hyaluronan-coated ELISA plate. The unbound b-HABP remaining in the sample could then bind to the hyaluronan-coated plate and was detected by incubation with 0.5 μg/ml of peroxidase-labeled streptavidin followed by a peroxidase substrate consisting of H_2O_2 and azinobis (3-ethyl-benzthiazoline sulfonic acid) in 0.1 M Na citrate (pH 5.0). The plate was read at A^{405}, and the concentration of hyaluronan in the samples was calculated from a standard curve.

The expression of CD44 by the vector-TSU and HAS3-TSU cells was examined by Western blotting. For this, both low- and high-density cultures were harvested with EDTA in PBS, and equivalent amounts of protein were dissolved in Laemmli sample buffer under nonreducing conditions and electrophoresed on a 10% SDS polyacrylamide gel. The resulting gel was electrophoretically transferred to a sheet of nitrocellulose and stained for CD44 using the BU52 monoclonal antibody (The Binding Site, Birmingham, United Kingdom) as described previously (24).

Anchorage-dependent Growth. Aliquots of medium (10% calf serum, 90% DMEM) containing 5000 transfected cells were added to 24-well dishes. At various times, the cells were harvested in 5 mM EDTA in PBS, and the cell number was determined with a Coulter counter. In some experiments, the cells were grown in the presence of 2 to 200 μg/ml of high molecular weight hyaluronan (Lifecore Biomedical, Chaska, MN) for 7 days.

Colony Formation. Vector-TSU or HAS3-TSU cells (20,000) were suspended in 1 ml of 0.36% agarose, 10% fetal bovine serum, 90% DMEM and then immediately placed on top of a layer of 0.6% solid agarose with 10% fetal bovine serum, 90% DMEM. Two weeks later, the number of colonies larger

than 50 μm in diameter was quantified using an Omnicon Image Analysis system (Imaging Products International, Chantilly, VA).

Endothelial Cell Proliferation and Migration. For the proliferation assay, 2×10^3 ABAE cells were subcultured into 96-well plates and allowed to grow overnight. The next day, the media was replaced with 150 μl of 1% calf serum, 99% DMEM along with 50 μl of conditioned medium from either vector-TSU or HAS3-TSU cells. After 36 h, 0.3 μCi of [^{3}H]thymidine was added to each well, and 8 h later the cells were processed with an autoharvester. The incorporated [^{3}H]thymidine was determined with a β-counter.

For the migration assay, 25-μl aliquots of 10% FCS, 90% DMEM containing 5×10^3 ABAE cells were added to bottom wells of a 48-well Boyden chamber (Nucleopore, Pleasanton, CA) and then covered with a nucleopore membrane (5-μm pore size) coated with 0.1 mg/ml gelatin (25). The top well chamber was assembled and inverted for 2 h to allow the cells to adhere to the bottom side of membrane and then turned upright. Conditioned medium (50 μl) from either the vector-TSU or HAS3-TSU cells was added to top wells of the chamber and incubated for 2 h. The membrane was removed, the bottom side was carefully wiped to remove cells that had not migrated, and then the cells on the topside were stained with Hema 3 (Biochemical Science, Swedenboro, NJ). The membrane was placed on a slide, and the number of cells that had migrated to the topside were counted in 10 random high-powered fields.

Tumor Growth and Metastasis Assay. Two assay systems were used to determine tumor growth *in vivo*. In the first assay, 2×10^6 vector-TSU and

```
                        G TGC GTT CGC GGC TGC TTT GAC CTG GTG GGC GCC GCC TCC
GGC ACT GCA CCG AGG CGG GGC GCC AGC GCC CAG GTT GCT GGG CTG GCC TTG GCG CCC CCT
TCC CCT ACC CAG AGC GCA GGC AGG CAG GGG GGT CCC GCC GCG CCC CTT CAG CAT ATG CCG160
                                                                     M   P    2
GTG CAG CTG ACG ACA GCC CTG CGT GTG GTG GGC ACC AGC CTG TTT GCC CTG GCA GTG CTG 220
 V   Q   L   T   T   A   L   R   V   V   G   T   S   L   F   A   L   A   V   L   22
GGT GGC ATC CTG GCA GCC TAT GTG ACG GGC TAC CAG TTC ATC CAC ACG GAA AAG CAC TAC 280
 G   G   I   L   A   A   Y   V   T   G   Y   Q   F   I   H   T   E   K   H   Y   42
CTG TCC TTC GGC CTG TAC GGC GCC ATC CTG GGC CTG CAC CTG CTC ATT CAG AGC CTT TTT 340
 L   S   F   G   L   Y   G   A   I   L   G   L   H   L   L   I   Q   S   L   F   62
GCC TTC CTG GAG CAC CGG CGC ATG CAA CGT GCC GGC CAG GCC CTG AAG CTG CCC TCC CCG 400
 A   F   L   E   H   R   R   M   Q   R   A   G   Q   A   L   K   L   P   S   P   82
CGG CGG GGC TCG GTG GCA CTG TGC ATT GCC GCA TAC CAG CAG GAC CCT GAC TAC TTG CGC 460
 R   R   G   S   V   A   L   C   I   A   A   Y   Q   E   D   P   D   Y   L   R  102
AAG TGC CTG CGC TCG GCC CAG CGC ATC TCC TTC CCT GAC CTC AAG GTG GTC ATG GTG GTG 520
 K   C   L   R   S   A   Q   R   I   S   F   P   D   L   K   V   V   M   V   V  122
GAT GGC AAC CGC CAG GAG GAC GCC TAC ATG CTG GAC ATC TTC CAC GAG GTG CTG GGC GGC 580
 D   G   N   R   Q   E   D   A   Y   M   L   D   I   F   H   E   V   L   G   G  142
ACC GAG CAG GCC GGC TTC TTT GTG TGG CGC AAC TTC CAT GAG GCA GGC GAG GGT GAG GAG 640
 T   E   Q   A   G   F   F   V   W   R   S   N   F   H   E   A   G   E   G   E  162
ACG GAG GCC AGC CTG CAG GAG GGC ATG GAC CGT GTG CGG GAT GTG GTG CGG GCC AGC ACC 700
 T   E   A   S   L   Q   E   G   M   D   R   V   R   D   V   V   R   A   S   T  182
TTC TCG TGC ATC ATG CAG AAG TGG GGA GGC AAG CGC GAG GTC ATG TAC ACG GCC TTC AAG 760
 F   S   C   I   M   Q   K   W   G   G   K   R   E   V   M   Y   T   A   F   K  202
GCC CTC GGC GAT TCG GTG CAT GAC TAC ATC CAG GTG TGC GAC TCT GAC ACT GTG CTG GAT CCA 820
 A   L   G   D   S   V   D   Y   I   Q   V   C   D   S   D   T   V   L   D   P  222
GCC TGC ACC ATC GAG ATG CTT CGA GTC CTG GAG GAC GAT CCC CAA GTA GGG GGA GTC GGG 880
 A   C   T   I   E   M   L   R   V   L   E   E   D   P   Q   V   G   G   V   G  242
GGA GAT GTC CAG ATC CTC AAC AAG TAC GAC TCA TGG ATT TCC TTC CTG AGC AGC GTG CGG 940
 G   D   V   Q   I   L   N   K   Y   D   S   W   I   S   F   L   S   S   V   R  262
TAC TGG ATG GCC TTC AAC GTG GAG CGG GCC TGC CAG TCC TAC TTT GGC TGT GTG CAG TGT1000
 Y   W   M   A   F   N   V   E   R   A   C   Q   S   Y   F   G   C   V   Q   C  282
ATT AGT GGG CCC TTG GGC ATG TAC CGC AAC AGC CTC CTC CAG CAG TTC CTG GAG GAC TGG1060
 I   S   G   P   L   G   M   Y   R   N   S   L   L   Q   Q   F   L   E   D   W  302
TAC CAT CAG AAG TTC CTA GGC AGC AAG TGC AGC TTC GGG GAT GAC CGG CAC CTC ACC AAC1120
 Y   H   Q   K   F   L   G   S   K   C   S   F   G   D   D   R   H   L   T   N  322
CGA GTC CTC AGC CTT GGC TAC CGA ACT AAG TAT ACC GGC CGC TCC AAG TGC CTC ACA GAG1180
 R   V   L   S   L   G   Y   R   T   K   Y   T   A   R   S   K   C   L   T   E  342
ACC CCC ACT AAG TAC CTC CGG TGG CTC AAC CAG CAA ACC CGC TGG AGC AAG TCT TAC TTC1240
 T   P   T   K   Y   L   R   W   L   N   Q   Q   T   R   W   S   K   S   Y   F  362
CGG GAG TGG CTC TAC AAC TCT CTG TGG TTC CAT AAG CAC CAC CTC TGG ATG ACC TAC GAG1300
 R   E   W   L   Y   N   S   L   W   F   H   K   H   H   L   W   M   T   Y   E  382
TCA GTG GTC ACG GGT TTC TTC CCC TTC TTC CTC ATT GCC ACG GTT ATA CAG CTT TTC TAC1360
 S   V   V   T   G   F   F   P   F   F   L   I   A   T   V   I   Q   L   F   Y  402
CGG GGC CGC ATC TGG AAC ATT CTC CTC TTC CTG CTG ACG GTG CAG CTG GTG GGC ATT ATC1420
 R   G   R   I   W   N   I   L   L   F   L   L   T   V   Q   L   V   G   I   I  422
AAG GCC ACC TAC GCC TGC TTC CTT CGG GGC AAT GCA GAG ATG ATC TTC ATG TCC CTC TAC1480
 K   A   T   Y   A   C   F   L   R   G   N   A   E   M   I   F   M   S   L   Y  442
TCC CTC CTC TAT ATG TCC AGC CTT CTG CCG GCC AAG ATC TTT GCC ATT GCT ACC ATC AAC1540
 S   L   L   Y   M   S   S   L   L   P   A   K   I   F   A   I   A   T   I   N  462
AAA TCT GGC TGG GGC ACC TCT GGC CGA AAA ACC ATT GTG GTG AAC TTC ATT GGC CTC ATT1600
 K   S   G   W   G   T   S   G   R   K   T   I   V   V   N   F   I   G   L   I  482
CCT GTG TCC ATC TGG GTG GTG GCA GTT CTC CTG GGA GGG CTG GCC TAC ACA GCT TAT TGC CAG1660
 P   V   S   I   W   V   V   A   V   L   L   G   G   L   A   Y   T   A   Y   C   Q  502
GAC CTG TTC AGT GAG ACA GAG CTA GCC TTC CTT GTC TCT GGG GCT ATA CTG TAT GGC TGC1720
 D   L   F   S   E   T   E   L   A   F   L   V   S   G   A   I   L   Y   G   C  522
TAC TGG GTG GCC CTC CTC ATG CTA TAT CTG GCC ATC ATC GCC CGG CGA TGT GGG AAG AAG1780
 Y   W   V   A   L   L   M   L   Y   L   A   I   I   A   R   R   C   G   K   K  542
CCG GAG CAG TCA AGC TTG GCT TTT GCT GAG GTG TGA CAT GGC CCC CAA GCA GAG CGG GTA1840
 P   E   Q   S   S   L   A   F   A   E   V   *                                  553
AAG TGC AAT GGG TAA GGG AGG GAA GGG GAA TGG AAG AGA AAA GAC AGG GTG GGA GGG AGG1900
AGG GAG TGC TGT GTT TTA GTC TCT TAA TGG TCC AAA GGA CAA ATC TAA AAT GCA AAG AAC1960
GGT GAT GTA GTA TGG CCT GAC AGC TCT GTT TA                                    1992
```

Fig. 1. Nucleotide sequence and derived amino acid sequence of human HAS3. The open reading frame of human HAS3 consists of 1659 bp coding for 553 amino acids. The signal peptide (first 27 amino acids) and the six transmembrane domains are *underlined*. Between the first transmembrane domain (amino acids 43 to 65) and the second transmembrane domain (amino acids 384 to 402) there is a stretch of 319 amino acids located outside of the plasma membrane, which is probably the major functional region for the synthase activity. The remaining 170 amino acids in the COOH terminus (amino acids 384 to 553) contain five transmembrane domains that can form loops that span the plasma membrane. The GenBank accession no. is AF234839.

Fig. 2. Comparison of the human HAS3 with other members of the HAS family. Human HAS3 is about 53% identical to HAS1, 67% identical to HAS2 of both human and mouse (*m*), and 96% identical to mouse HAS3.

HAS3-TSU cells were placed on the chorioallantoic membranes of 10-day-old chicken embryos (15 eggs/group) and incubated at 37°C for 5 days. The tumor masses that grew on the chorioallantoic membranes were removed, photographed, and weighed. In the second assay system, the transfected cells were injected s.c. into 5-week-old male nude mice (2×10^6 cells/site; five mice/group), and the size of the xenografts was measured twice a week. At the end of 3 weeks, the mice were sacrificed, and the xenografts were photographed, weighted, and then fixed with 3.7% formaldehyde or frozen in liquid nitrogen for immunohistochemical staining.

To examine experimental metastasis, 5×10^5 vector-TSU and HAS3-TSU cells were injected into the tail veins of 5-week-old nude mice (five mice/group). Three weeks later, the mice were sacrificed, and the lungs were examined under a dissecting microscope for metastases.

Histological Staining. To stain cultured cells for hyaluronan, the transfected cells were seeded into an 8-well chamber slide (Nunc, Naperville, IL) and allowed to grow to confluence. After fixation in 3.7% formaldehyde for 5 min, the cells were washed and stained with 10 μg/ml b-HABP in 10% calf serum, 90% PBS, followed by 4 μg/ml of peroxidase-conjugated streptavidin and finally a substrate consisting of 3-amino-9-ethyl-carbazole and H_2O_2 that gives a dark red reaction product (23).

To stain xenografts for hyaluronan, the tissue was fixed with formaldehyde, embedded in paraffin, and cut into 5-μm thick sections. After the removal of the paraffin, the sections were processed as described above. After the immunoperoxidase reaction step, the sections were counter-stained with Mayer's hematoxylin and then preserved with Crystal/Mount (Biomeda, Foster City, CA).

To stain for endothelial cells, samples of the xenografts were rapidly frozen, cut into 10-μm thick sections, fixed in acetone, and air-dried. The sections were incubated sequentially with: (*a*) a 1:30 dilution of rat antimouse CD31 (PharMigen, San Diego, CA) in 10% calf serum, 90% PBS for 1 h; (*b*) avidin-biotin complex method reagents for rat IgG (ABC kits; Biomeda); (*c*) a peroxidase substrate consisting of H_2O_2 and 3-amino-9-ethyl-carbazole; and (*d*) counter-stained with Mayer's hematoxylin. The numbers of immunopositive spots corresponding to small blood vessels were counted in 10 random fields of three samples from each group.

Statistical Analysis. The mean and SE were calculated from the raw data and then subjected to Student's *t* test. The $P < 0.05$ was regarded as statistically significant.

RESULTS

Cloning and Characterization of Human HAS3. The full-length cDNA for HAS3 was cloned from a cDNA library of human brain using a probe consisting of a known partial sequence of the gene. The open reading frame contained 1659 bp coding for 553 amino acids and is shown in Fig. 1. The HAS3 protein had a deduced molecular weight of about 63,000 and a pI of 8.70. The first 27 amino acids represented
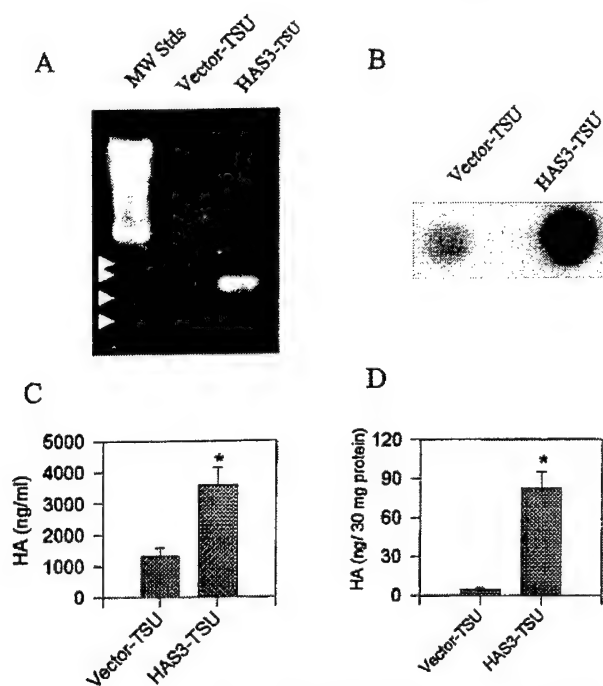
Fig. 3. Analysis of vector-TSU and HAS3-TSU cells for HAS3 mRNA and hyaluronan production. *A*, for the analysis of HAS3 message, RNA was extracted from the cultured cells and subjected to RT-PCR as described in "Materials and Methods." Agarose gel electrophoresis of the reaction products showed that the HAS3-TSU cells contained a prominent band of approximately 280 bp that was absent from the vector-TSU cells. The positions of markers for 100 through 400 bp are indicated by the *arrowheads* in the first *lane*. *B*, for the analysis of hyaluronan production, conditioned media from the transfected cells was applied to nitrocellulose using a dot blot apparatus and stained for hyaluronan using b-HABP, followed by peroxidase-labeled streptavidin and a chemiluminescence reagent. The dots represent the hyaluronan in conditioned media of vector-TSU cells (*left*) and HAS3-TSU cells (*right*). *C* and *D*, the amount of hyaluronan in conditioned media and cell lysates as determined by an ELISA are shown respectively. The increase of hyaluronan in conditioned media and lysates from HAS3-TSU cells as compared with the vector-TSU cells was statistically significant ($P < 0.05$).

the signal peptide (the cleavage site is between ILA and AY). There were six transmembrane sequences, one in the NH_2 terminus and five in the COOH terminus. Between the first transmembrane sequence (from amino acid 43 to 65) and second transmembrane sequence (from amino acid 384 to 402), there was a stretch of 319 amino acids located outside of plasma membrane, which appeared to be the major functional region for polysaccharide synthesis. The 170 amino acids in the COOH terminus (from amino acid 384 to 553) contained five transmembrane domains that can form loops spanning in and out of the plasma membrane. A potential *N*-glycosylation site was present at amino acid position 462, a glycosaminoglycan attachment site at position 464, and several phosphorylation sites for tyrosine kinase, casein kinase, protein kinase C, and cyclic AMP- and cyclic GMP-dependent protein kinases. HAS3 also contained seven hyaluronan-binding motifs of $B(X_7)B$ in which B is either R or K, and X_7 contains no acidic residues and at least one basic amino acid (26). Similar domains are present in other hyaluronan-binding proteins such as RHAMM, CD44, hyaluronidase, link protein, aggrecan, human GHAP, and TSG-6. Fig. 2 shows that compared with related enzymes, human HAS3 was about 53% identical to HAS1 (both human and mouse forms), 67% identical to HAS2, and 96% identical to mouse HAS3. These results are consistent with earlier studies of this and related genes (13–19).

Overexpression of Hyaluronan in TSU Cells Transfected with HAS3. To examine the role of HAS3 in tumor progression, the cloned cDNA was inserted into a mammalian expression vector (pcDNA3) under the control of a cytomegalovirus promoter and then

transfected into TSU cells (human prostate cancer). To avoid complications associated with clonal variations, all of the clones (>100) that survived in 1 mg/ml of Geneticin (G418) were pooled and expanded for experimental analysis throughout this study. The presence of HAS3 message in the transfected cells was examined by RT-PCR as described in "Materials and Methods." When analyzed by agarose gel electrophoresis (Fig. 3*A*), the HAS3-TSU cells gave rise to a PCR product of approximately 280 bp corresponding to HAS3, whereas no such band was detected in the vector-TSU cells. In addition, no reaction product of 314 bp was apparent, indicating that the message for HAS1 was absent from these cells.

The production of hyaluronan by the transfected cells was initially examined by dot blot analysis. As showed in Fig. 3*B*, conditioned medium from HAS3-TSU cells contained a significantly greater amount of hyaluronan than that from vector-TSU cells. To quantitatively measure the hyaluronan, a competitive enzyme-linked assay was performed. Fig. 3, *C* and *D* show that both conditioned medium and lysates of HAS3-TSU cells contained greater amounts of hyaluronan as compared with those of the control vector-TSU cells. However, there was no obvious difference in the level of CD44, a cell surface receptor for hyaluronan, on the two cell types at either low or high density as determined by Western blotting (data not shown). Taken together, these results indicate that the transfection of TSU cells with cDNA for HAS3 stimulated their production of hyaluronan.

HAS3 Promotes Cell Growth at High Densities. We then compared the growth rates of the vector-TSU and HAS3-TSU cells. For this, the transfected cells were subcultured at similar starting densities, and at various times thereafter the cells were harvested and enumerated with a Coulter counter. Fig. 4*A* shows that during the first 4 days, there was no obvious difference in the proliferation rates of the vector-TSU and HAS3-TSU cells. However, after day 5, the HAS3-TSU cells began to proliferate at a faster rate than the vector-TSU cells. Thus, at high densities, the HAS3-transfected cells grew at a faster rate. This conclusion was also suggested by our recent finding that transfection of MDA-231 human breast cancer cells with anti-sense to HAS3 results in decreased expression of hyaluronan and inhibition of their growth at high densities.[4] Together, these results indicate that HAS3 plays a role in cell proliferation at high densities.

Cultures of the vector-TSU and HAS3-TSU cells were then compared with respect to their patterns of growth and hyaluronan staining. As shown in Fig. 4*B* (*top*), the vector-TSU cells displayed a cobble-stone appearance indicative of contact inhibition of growth with relatively little staining of pericellular hyaluronan. In contrast, the HAS3-TSU cells (Fig. 4*B*, *bottom*) appeared to have lost contact-inhibition of growth, forming numerous multilayered clusters of cells, which were associated with most of the hyaluronan staining. In addition, the HAS3-TSU cells displayed an enhanced ability to form colonies in soft agar as compared with the vector-TSU cells (Fig. 4*C*). Thus, at high densities, the HAS3-transfected cells grew at a faster rate, presumably because they had partially lost contact inhibition of growth.

Conditioned Medium from HAS3-TSU Stimulated the Proliferation and Migration of Endothelial Cells. Because several studies (27–29) reported that hyaluronan can modulate angiogenesis, we examined the effects of conditioned medium from HAS3-TSU cells on the behavior of cultured endothelial cells. When conditioned medium from HAS3-TSU cells was added to the medium of ABAE cells, it stimulated their proliferation by 66% as compared with that from vector-TSU cells (Fig. 5*A*). Furthermore, conditioned medium from the HAS3-TSU also stimulated the migration of ABAE cells through

---

[4] Unpublished data.
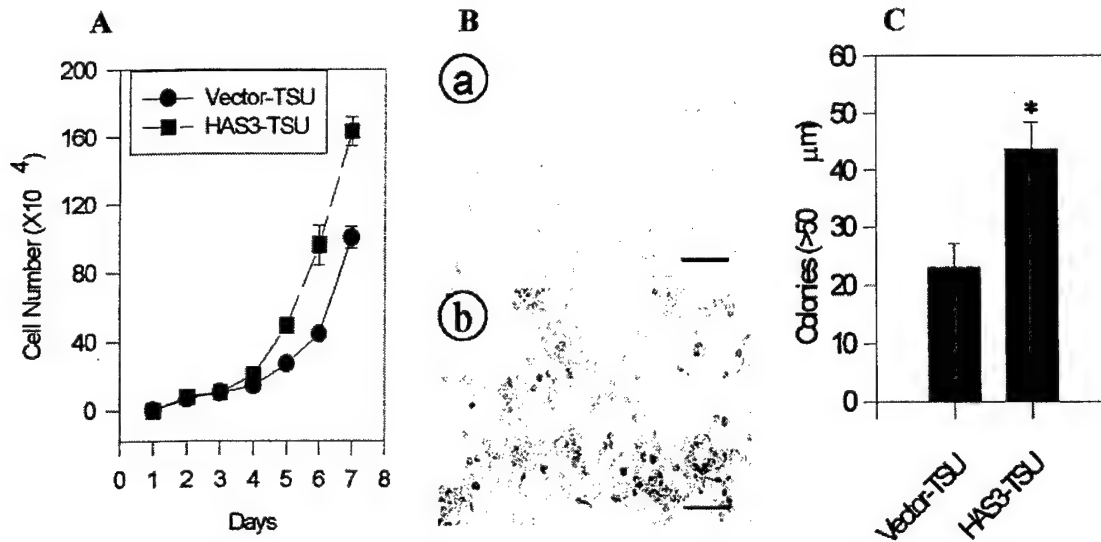
A

B

C

Fig. 4. *In vitro* growth pattern of vector-TSU and HAS3-TSU cells. *A*, cell growth curves for the transfected TSU cells are shown. The cells were plated in 24-well dishes, and the cell number was determined at the indicated times. Although the rate of cell growth was the same at low densities, at higher densities, the HAS3-TSU cells grew faster than the vector-TSU cells. Three independent experiments yielded similar results. *B*, transfected cells at high density were stained for hyaluronan. The transfected cells were grown to confluence, briefly fixed in formaldehyde, and stained for hyaluronan with b-HABP, followed by peroxidase-labeled streptavidin and finally a substrate for peroxidase that gives a red color. The vector-TSU cells (*part a*) formed a confluent monolayer with little hyaluronan staining, whereas the HAS3-TSU cells (*part b*) formed numerous multilayered clusters that stain for hyaluronan (*bar*, 100 μm). *C*, anchorage-independent growth of the transfected cells is shown. Equal numbers of vector-TSU and HAS3-TSU cells were cultured in soft agar for 2 weeks, and the number of colonies were counted with Omnicon Image Analysis system. The HAS3-TSU cells formed a greater number of colonies larger than 50 μm than did the vector-TSU cells (*, $P < 0.05$). This experiment was performed in triplicate.

nucleopore filters by more than 300% as compared with conditioned medium from control cells (Fig. 5*B*). These results further suggest that the hyaluronan produced by HAS3-TSU cells could exert a stimulatory effect on endothelial cells.

The Growth of Transfected Cells on the Chicken Chorioallantoic Membrane. To determine whether the increased growth rate of HAS3-TSU cells *in vitro* also occurred *in vivo*, we examined their growth on the chorioallantoic membranes of chicken eggs. In this experiment, equal numbers of vector-TSU and HAS3-TSU cells were placed on the chorioallantoic membranes of 10-day-old chicken embryos and allowed to grow for 5 days. The xenografts showed a striking divergence in morphology. The vector-TSU cells formed rounded, nodular xenografts that grew out of the membrane surface, with necrotic tissue in the center, whereas the HAS3-TSU cells gave rise to xenografts with a dispersed morphology within the membrane and without any obvious signs of necrosis. As shown in Fig. 6, *A* and *B*, the HAS3-TSU xenografts were significantly larger than those of the vector-TSU cells. Histological examination of the xenografts revealed that, whereas the vector-TSU cells were compact, the HAS3-TSU cells were more dispersed with increased intercellular spaces (data not shown). These results suggested that overexpression of hyaluronan enhanced the tumor growth on the chorioallantoic membrane system.

HAS3 Promotes the Primary Growth of TSU Cells but Not Metastasis in Nude Mice. The *in vivo* growth characteristics of these cells were further examined by injecting them s.c. into nude mice. After 2 weeks, the xenografts formed by HAS3-TSU cells grew at a faster rate and appeared to be more vascularized than the control cells. After 3 weeks of growth, the HAS-3 xenografts were three times larger than those formed by the vector-TSU cells (Fig. 7, *A* and *B*), suggesting that HAS3 promotes the growth of TSU tumor cells in mice. These results are consistent with those obtained from the chicken chorioallantoic membrane system.

However, when transfected cells were injected into the tail veins of nude mice (five mice/group), no lung metastases were detected with

either cell type. Thus, the overexpression of hyaluronan by itself is not sufficient to induce metastatic behavior in TSU cells.

Increased Extracellular Hyaluronan and Angiogenesis in HAS3-TSU Xenografts. The xenografts from nude mice were processed for histology, and the resulting sections were stained for hyaluronan (Fig. 8*A*). Although the xenografts varied from region to region, in general, the cells in the vector-TSU xenografts were relatively homogeneous and compact, and most of the hyaluronan appeared to be present in the cytoplasm of the cells (Fig. 8*A*). In contrast, the HAS3-TSU cells formed small clusters or nests of cells that were
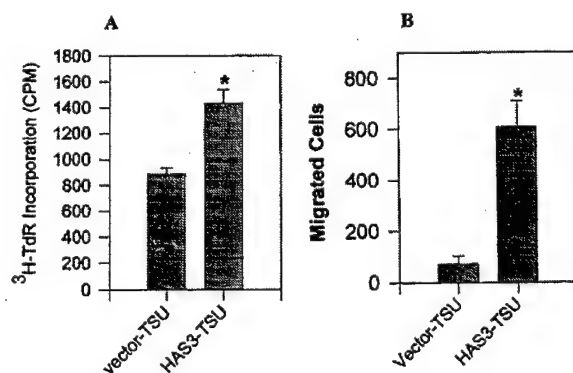
A   **B**

Fig. 5. Effect of conditioned media from vector-TSU and HAS3-TSU cells on endothelial cells. *A*, effects of conditioned media on the proliferation of endothelial cell are demonstrated. ABAE cells were cultured for 36 h in the presence of conditioned media from either vector-TSU or HAS3-TSU cells, pulsed with [^{3}H]thymidine for 8 h, harvested, and processed for incorporated radioactivity. The conditioned media from HAS3-TSU cells stimulated the ABAE cells to a greater extent than that from vector-TSU cells. *B*, effects of conditioned medium on the migration of endothelial cells is shown. Aliquots containing 5×10^3 ABAE cells were added to bottom wells of a 48-well Boyden chamber, covered with a nucleopore membrane, and then treated with 50 μl of conditioned medium for 2 h. The membrane was stained with Hema 3 and placed on a slide, and the migrated cells were counted in 10 random fields. Conditioned medium from HAS3-TSU cells significantly increased the migration of the endothelial cells as compared with that from the vector-TSU cells ($P < 0.05$).
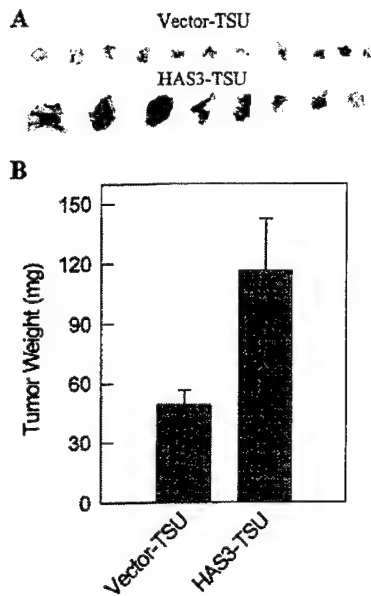
A

Vector-TSU

HAS3-TSU

B

Fig. 6. Growth of transfected TSU cells on the chicken chorioallantoic membrane. Samples of vector-TSU and HAS3-TSU cells (2 × 10⁶ cells) were placed on the chorioallantoic membranes of 10-day-old chicken embryos (15 eggs/group), incubated at 37°C for 5 days, and then photographed. A, the xenografts of vector-TSU cells (top row) and HAS3-TSU cells (bottom row) from the chorioallantoic membrane are shown. The vector-TSU xenografts formed compact nodules, whereas the HAS3-TSU xenografts were more spread out and larger. B, the weights of the HAS3-TSU xenografts were significantly greater than that of the vector-TSU cells ($P < 0.05$).

surrounded by a matrix rich in hyaluronan (Fig. 8A). Such structures were not observed in the control-TSU xenografts.

The extent of angiogenesis in these xenografts was examined by staining for mouse endothelial cells using antibodies to CD31. Fig. 8B shows that there was strong positive staining in HAS3-TSU xenografts as compared with the control vector-TSU xenografts. The number of vessels in 10–15 random fields was significantly higher in the HAS3-TSU xenografts than in the control xenografts (Fig. 8C). This suggests that increased levels of hyaluronan can stimulate angiogenesis in mice, and this may, in part, account for the faster growth rate of tumors formed by HAS3-TSU cells.

DISCUSSION

In this study, we have characterized human HAS3 with regard to both its structure and its function in tumor progression. On the basis of its deduced amino acid sequence, HAS3 shares significant homology with HAS1 and HAS2, containing a signal peptide as well as six transmembrane regions strongly suggesting that it is associated with the plasma membrane. Its enzymatic activity was demonstrated by the fact that TSU cells transfected with expression vectors for HAS3 produced larger amounts of hyaluronan as determined by histochemical staining, dot blot analysis, and quantitative ELISA. These findings are consistent with earlier studies of HAS proteins (12–19).

This study also suggested that stimulation of hyaluronan synthesis in TSU cells by transfecting them with HAS3 expression vectors enhanced their growth both in chicken embryos and in nude mice. This enhanced tumor growth appeared to be attributable to two distinct mechanisms. The first involved a direct effect on the tumor cells themselves, as indicated by the fact that in tissue culture, HAS3-transfected cells grew at a faster rate at high density. The second mechanism promoting tumor growth rate resulted from an increase in vascularization, as reflected by the greater density of blood vessels in xenografts from nude mice. Together, these two factors contribute to the increased tumor growth rate.

At present, we believe that the effects of HAS3 transfection on TSU cell phenotype are a direct consequence of increased hyaluronan synthesis. Along these lines, it is important to note that HAS3 overexpression increases the production of both secreted and cell-associated hyaluronan. These two pools of hyaluronan may have different effects on cell behavior. This was suggested by preliminary experiments in which we found that the addition of high molecular weight hyaluronan to cultures of vector-TSU or HAS3-TSU cells had no obvious effect on their growth rates (data not shown). We believe that under these specific conditions, free hyaluronan of high molecular weight did not affect the behavior of these cells. Rather, we believe that it was the cell-associated fraction of hyaluronan induced by HAS3 that played a more important role in stimulating cell growth. However, we cannot eliminate the possibility that hyaluronan of the appropriate size and concentration may indeed influence the behavior of TSU cells, similar to the effects that it has on endothelial cells (27, 28). It is also possible that HAS3 may have effects on the TSU cells independent of its function to promote hyaluronan synthesis; e.g., HAS3 could influence the interaction of the plasma membrane with elements of the cytoskeleton and thereby alter cell behavior.

The hyaluronan on the surface of cultured cells can form a pericellular coat that can be directly visualized by its ability to exclude small particles such as erythrocytes (30). In the case of rat fibrosarcoma cells, this coat is composed of small, microvilli-like projections that extend out from the surface of the cells to which the hyaluronan is attached (31). This pericellular coat could stimulate the growth of cells by several different mechanisms. One possible mechanism is that it disrupts intercellular junctions and thereby allows the cells to detach from the substrate so that they can divide and occupy new space (32–34). This would allow cells to overcome contact inhibition of growth that is characteristic of TSU cells and allow them to from multilayers at high-density cultures as we have observed. Another possibility is that the hyaluronan interacts with receptors on the surfaces of cells such as CD44 or RHAMM to influence their migratory and proliferative behavior (35, 36).

Extracellular hyaluronan can also stimulate cell proliferation by

A

Vector-TSU

HAS3-TSU

B

Fig. 7. Xenografts formed by transfected TSU cells in nude mice. A, the appearance of xenografts formed in nude mice is shown. Mice received injections of 2 × 10⁶ vector-TSU cells (top) or HAS3-TSU cells (bottom), and the xenografts were harvested 21 days later. The HAS3-TSU xenografts were larger than those of the vector-TSU cells. B, the weights of the HAS3-TSU xenografts were significantly greater than that of the vector-TSU ($P < 0.05$).
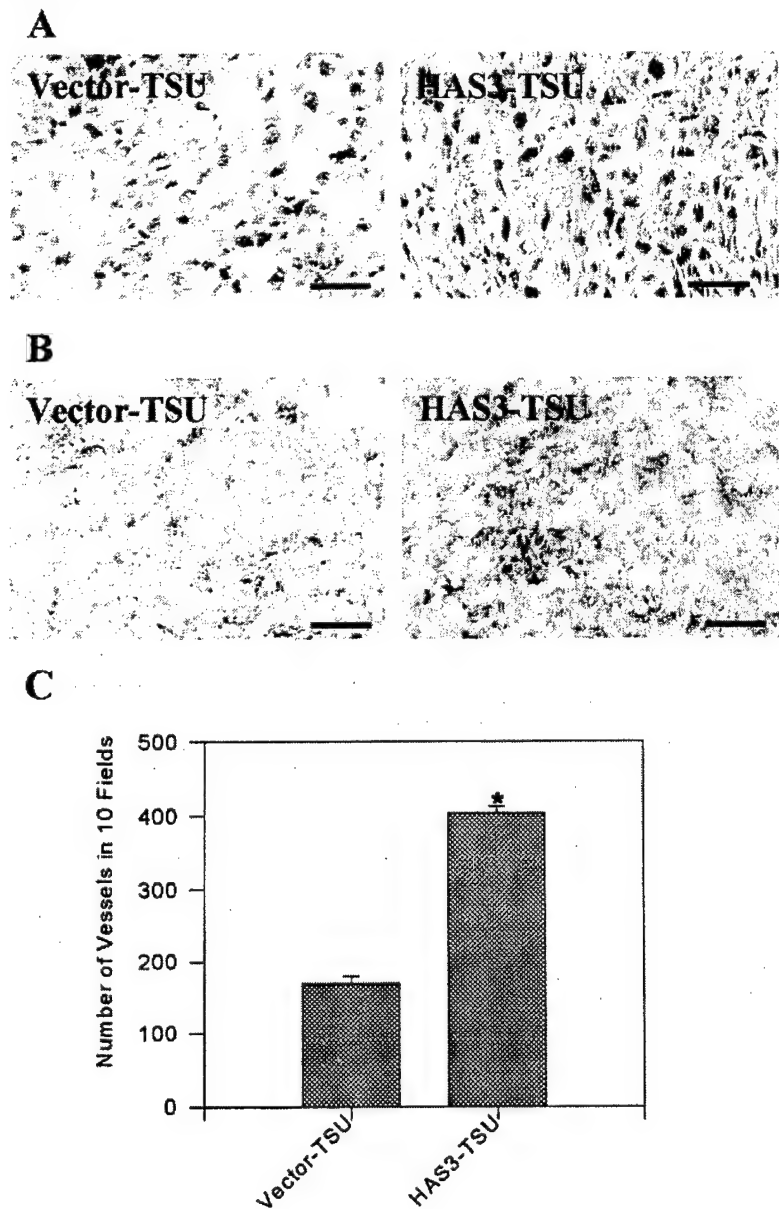
A

B

C

Fig. 8. Staining of xenografts for hyaluronan and endothelial cells. *A*, paraffin sections of vector-TSU and HAS3-TSU xenografts from nude mice were stained for hyaluronan (*red*) and counter-stained with hematoxylin (*blue*). A representative section of a vector-TSU xenograft shows that most of the hyaluronan staining was associated with the cytoplasm of the cells, whereas in a similar section from a HAS3-TSU xenograft, the cells were present in small clusters, surrounded by a stroma rich in hyaluronan. Although the microscopic morphology of the xenografts varied from region to region, the hyaluronan-rich stroma was prevalent in the HAS3-TSU xenografts and absent from the vector-TSU xenografts. *Bar*, 50 μm. *B*, cryostat sections of the xenografts were stained for endothelial cells using an antibody against mouse CD31. Representative fields show that xenografts formed from HAS3-TSU cells have a higher concentration of endothelial cells than those from vector-TSU cells. *Bar*, 100 μm. *C*, the number of blood vessels in 10 random fields from three samples of each group are shown. The HAS3-TSU xenografts had a significantly higher concentration of blood vessels than that of the vector-TSU cells ($P < 0.05$).

increasing the flow of nutrients. Indeed, the extracellular hyaluronan apparent in xenografts of HAS3-TSU cells in nude mice could serve as conduits through which nutrients diffuse to support cells located some distance from the blood supply and thus facilitate their growth. In the xenografts of vector-TSU cells that lacked these hyaluronan rich spaces, the tumor cells formed a continuous mass and were more susceptible to necrosis. Along these lines, extracellular hyaluronan is prominent in the lower regions of most, if not all, stratified epithelium, where it is believed to maintain spaces so that nutrients can diffuse to the more superficial epithelial cells (37, 38).

Hyaluronan also appeared to promote vascularization that is clearly important in regulating tumor growth (39, 40). This was indicated by our observation that xenografts of HAS3-TSU cells formed in nude mice had a greater density of blood vessels than did control xenografts. Part of this increased vascularization may be attributable to the pericellular spaces generated by the hyaluronan that provides space that facilitates the invasion of endothelial cells. In addition, the hyaluronan itself can stimulate the migration of endothelial cells. This was also indirectly suggested by experiments showing that condi-

tioned media from the HAS3-transfected cells stimulated the growth and migration of cultured endothelial cells. This is consistent with the earlier studies of West *et al.* (27, 28) who have shown that oligosaccharide fragments of hyaluronan stimulated the formation of new blood vessels in the chorioallantoic membrane of chicken embryos.

Although the results of this study suggest that overexpression of HAS3 in TSU prostate cancer cells promotes their tumorigenicity, there are some aspects that appear to contradict the findings of other studies; *e.g.*, although we found that TSU transfectants grew faster in culture, Kosaki *et al.* (20) found no such increase in the growth of HT1080 cells transfected with HAS2 under anchorage-dependent conditions; however, these cells did form larger colonies in suspension culture. We believe that this difference may be attributable in part to the different target cells that were used in these studies. The TSU cells used as targets in this study are of epithelial origin, whereas HT1080 cells are derived from a fibrosarcoma of connective tissue cells. This could also account for the differences seen with regard to growth behavior and the production of hyaluronan in the connective tissue and their ability to stimulate angiogenesis. Alternatively, the

differences could be attributed to the characteristics of the particular HASs that were used in these studies, because they differ with respect to both their synthetic activity as well as the size of the hyaluronan that they produce (16–18).

Another apparent discrepancy was our observation that transfection of TSU cells with HAS3 did not appear to stimulate their ability to form lung metastases in nude mice. In contrast, we had reported previously (3) that the levels of hyaluronan on the surface of B16 cells were directly correlated with their metastatic behavior. Similarly, Itano *et al.* (21) found that transfection of FM3A with HAS1 enhanced their metastatic properties. Again, we believe that these divergent results were attributable to the different cell types that were used as targets for transfection. In the case of B16 and FM3A, these cell lines originally possessed the ability to undergo metastasis, and stimulation of hyaluronan synthesis in these cells enhanced this innate property. In contrast, TSU cells appeared to lack this ability (at least in nude mice), and increased hyaluronan synthesis, by itself, is not sufficient to promote metastatic properties. Clearly, the process of metastasis is a complex phenomenon involving the collaboration of many molecules. Although the production of hyaluronan is one of the factors, it is not sufficient for tumor metastasis in the case of TSU cells.

In conclusion, the results of this study indicate that HAS3 expression plays a role in tumor progression and are consistent with earlier studies demonstrating a correlation between hyaluronan levels and tumorigenicity. Furthermore, the hyaluronan may be acting through several different mechanisms, including: (*a*) a direct effect on the growth of the tumor cells themselves; (*b*) the formation of extracellular conduits through which nutrients can flow; and (*c*) the stimulation of blood vessel growth. However, these effects depend upon the particular cell type and the specific environment. Given the complexity of the effects of hyaluronan, it may be difficult to predict exactly how it will influence the behavior of tumor cells. In the case of TSU cells, hyaluronan may be more of a facilitator of tumor growth rather than an instigator of metastasis.

REFERENCES

1. Toole, B. P., Biswas, C., and Gross, J. Hyaluronate and invasiveness of the rabbit V2 carcinoma. Proc. Natl. Acad. Sci. USA, *76:* 6299–6303, 1979.
2. Kimata, K., Honma, Y., Okayama, M., Oguri, K., Hozumi, M., and Suzuki, S. Increased synthesis of hyaluronic acid by mouse mammary carcinoma cell variants with high metastatic potential. Cancer Res., *43:* 1347–1354, 1983.
3. Zhang, L., Underhill, C. B., and Chen, L. Hyaluronan on the surface of tumor cells is correlated with metastatic behavior. Cancer Res., *55:* 428–433, 1995.
4. Marotta, M., D'Armiento, F. P., Martino, G., Donato, G., Nazzaro, A., Vecchione, R., and Rosati, P. Glycosaminoglycans in human breast cancer: morphological and biochemical study. Appl. Pathol., *3:* 164–169, 1985.
5. Coppes, M. J. Serum biological markers and paraneoplastic syndromes in Wilm's tumor. Med. Pediatr. Oncol., *21:* 213–221, 1993.
6. Horai, T., Nakamura, N., Tateshi, R., and Hattori, S. Glycosaminoglycans in human lung cancer. Cancer (Phila.), *48:* 2016–2021, 1981.
7. Roboz, J., Greaves, J., Silides, D., Chahinian, A. P., and Holland, J. F. Hyaluronic acid content of effusions as a diagnostic aid for malignant mesothelioma. Cancer Res., *45:* 1850–1854, 1985.
8. Kojima, J., Nakamura, N., Kanatani, M., and Omori, K. The glycosaminoglycans in human hepatic cancer. Cancer Res., *35:* 542–547, 1975.
9. Azumi, N., Underhill, C. B., Kagan, E., and Sheibani, K. A novel biotinylated probe specific for hyaluronate: its diagnostic value in diffuse malignant mesothelioma. Am. J. Surg. Pathol., *16:* 116–121, 1992.
10. Dahl, I. M. S., and Laurent, T. C. Concentration of hyaluronan in serum of untreated cancer patients reference to patients with mesothelioma. Cancer (Phila.), *62:* 326–330, 1988.
11. Frebourg, T., Lerebours, G., Delpech, B., Benhamou, D., Bertrand, P., Maingonnat, C., Boutin, C., and Nouvet, G. Serum hyaluronate in malignant pleural mesothelioma. Cancer (Phila.), *59:* 2104–2107, 1987.
12. Shyjan, A. M., Heldin, P., Butcher, E. C., Yoshino, T., and Briskin, M. J. Functional cloning of the cDNA for a human hyaluronan synthase. J. Biol. Chem., *271:* 23395–23399, 1996.
13. Watanabe, K., and Yamaguchi, Y. Molecular identification of a putative human hyaluronan synthase. J. Biol. Chem., *271:* 22945–22948, 1996.
14. Itano, N., and Kimata, K. Molecular cloning of human hyaluronan synthase. Biochem. Biophys. Res. Commun., *222:* 816–820, 1996.
15. Itano, N., and Kimata, K. Expression cloning and molecular characterization of HAS protein, a eukaryotic hyaluronan synthase. J. Biol. Chem., *271:* 9875–9878, 1996.
16. Spicer, A. P., Olson, J. S., and McDonald, J. A. Molecular cloning and characterization of a cDNA encoding the third putative mammalian hyaluronan synthase. J. Biol. Chem., *272:* 8957–8961, 1997.
17. Spicer, A. P., and McDonald, J. A. Characterization and molecular evolution of a vertebrate hyaluronan synthase gene family. J. Biol. Chem., *273:* 1923–1932, 1998.
18. Spicer, A. P., and Nguyen, T. K. Mammalian hyaluronan synthases: investigation of functional relationships *in vivo.* Biochem. Soc. Trans., *27:* 109–115, 1999.
19. Itano, N., Sawai, T., Yoshida, M., Lenas, P., Yamada, Y., Imagawa, M., Shinomura, T., Hamaguchi, M., Yoshida, Y., Ohnuki, Y., Miyauchi, S., Spicer, A. P., McDonald, J. A., and Kimata, K. Three isoforms of mammalian hyaluronan synthases have distinct enzymatic properties. J. Biol. Chem., *274:* 25085–25092, 1999.
20. Kosaki, R., Watanabe, K., and Yamaguchi, Y. Overproduction of hyaluronan by expression of the hyaluronan synthase Has2 enhances anchorage-independent growth and tumorigenicity. Cancer Res., *59:* 1141–1145, 1999.
21. Itano, N., Sawai, T., Miyaishi, O., and Kimata, K. Relationship between hyaluronan production and metastatic potential of mouse mammary carcinoma cells. Cancer Res., *59:* 2499–2504, 1999.
22. Chen, C., and Okayama, H. High-efficiency transformation of mammalian cells by plasmid DNA. Mol. Cell. Biol., *7:* 2745–2752, 1987.
23. Underhill, C. B., and Zhang, L. Analysis of hyaluronan using biotinylated hyaluronan-binding proteins. Methods Mol. Biol., *137:* 441–447, 1999.
24. Culty, M., Shizari, M., Nguyen, H. A., Clarke, R., Thompson, E. W., and Underhill, C. B. Degradation of hyaluronan and expression of CD44 by human breast cancer cell lines correlate with their invasive potential. J. Cell. Physiol., *160:* 275–286, 1994.
25. Falk, W., Goodwin, R. H., and Leonard, E. J. A 48-well micro chemotaxis assembly for rapid and accurate measurement of leukocyte migration. J. Immunol. Methods, *33:* 239–247, 1980.
26. Yang, B., Yang, B. L., Savani, R. C., and Turley, E. A. Identification of a common hyaluronan binding motif in the hyaluronan binding proteins RHAMM, CD44 and link protein. EMBO J., *13:* 286–296, 1994.
27. West, D. C., Hampson, I. N., Arnold, F., and Kumar, S. Angiogenesis induced by degradation products of hyaluronic acid. Science (Wash. DC), *228:* 1324–1326, 1985.
28. West, D. C., and Kumar, S. The effect of hyaluronate and its oligosaccharides on endothelial cell proliferation and monolayer integrity. Exp. Cell Res., *183:* 179–196, 1989.
29. Feinberg, R. N., and D. C. Beebe. Hyaluronate in vasculogenesis. Science (Wash. DC), *220:* 1177–1179, 1983.
30. Underhill, C. B., and Toole, B. P. Transformation-dependent loss of the hyaluronate-containing coats of cultured cells. J. Cell. Physiol., *110:* 123–128, 1982.
31. Koshiishi, I., Shizari, M., and Underhill, C. B. CD44 mediates the adhesion of platelets to hyaluronan. Blood, *84:* 390–396, 1994.
32. Brecht, M., Mayer, U., Schlosser, E., and Prehm, P. Increased hyaluronate synthesis is required for fibroblast detachment and mitosis. Biochem. J., *239:* 445–450, 1986.
33. Lark, M. W., and Culp, L. A. Selective solubilization of hyaluronic acid from fibroblast substratum adhesive sites. J. Biol. Chem., *257:* 14073–14080, 1982.
34. Abatangelo, G., Cortivo, R., Martelli, M., and Vecchia, P. Cell detachment mediated by hyaluronic acid. Exp. Cell Res., *137:* 73–78, 1982.
35. Zhang, S., Chang, M. C., Zylka, D., Turley, S., Harrison, R., and Turley, E. A. The hyaluronan receptor RHAMM regulates extracellular-regulated kinase. J. Biol. Chem., *273:* 11342–11348, 1998.
36. Bourguignon, L. Y., Shu, H., Shao, L., and Chen, Y. W. CD44 interaction with Tiam1 promotes Rac1 signaling and hyaluronic acid-mediated breast tumor migration. J. Biol. Chem., *275:* 1829–1338, 2000.
37. Alho, A. M., and Underhill, C. B. The hyaluronate receptor is preferentially expressed on proliferating epithelial cells. J. Cell Biol., *108:* 1557–1565, 1989.
38. Underhill, C. B. The interaction of hyaluronate with the cell surface: the hyaluronate receptor and the core protein. Ciba Found. Symp., *143:* 87–106, 1989.
39. Folkman, J. New perspectives in clinical oncology from angiogenesis research. Eur. J. Cancer, *32:* 2534–2539, 1996.
40. Folkman, J., and D'Amore, P. A. Blood vessel formation: what is its molecular basis? Cell, *87:* 1153–1155, 1996.

Metastatin: A Hyaluronan-binding Complex from Cartilage That Inhibits Tumor Growth[1]

Ningfei Liu,[2] Randall K. Lapcevich,[2] Charles B. Underhill, Zeqiu Han, Feng Gao, Glenn Swartz, Stacy M. Plum, Lurong Zhang,[2] and Shawn J. Green[2, 3]

Department of Oncology, Georgetown University Medical Center, Washington, D.C. 20007 [N. L., C. B. U., Z. H., F. G., L. Z.], and EntreMed, Inc., Rockville, Maryland 20902 [R. K. L., G. S., S. M. P., S. J. G.]

ABSTRACT

In this study, a hyaluronan-binding complex, which we termed Metastatin, was isolated from bovine cartilage by affinity chromatography and found to have both antitumorigenic and antiangiogenic properties. Metastatin was able to block the formation of tumor nodules in the lungs of mice inoculated with B16BL6 melanoma or Lewis lung carcinoma cells. Single i.v. administration of Metastatin into chicken embryos inhibited the growth of both B16BL6 mouse melanoma and iTSU human prostate cancer cells growing on the chorioallantoic membrane. The *in vivo* biological effect may be attributed to the antiangiogenic activity because Metastatin is able to inhibit the migration and proliferation of cultured endothelial cells as well as vascular endothelial growth factor-induced angiogenesis on the chorioallantoic membrane. In each case, the effect could be blocked by either heat denaturing the Metastatin or premixing it with hyaluronan, suggesting that its activity critically depends on its ability to bind hyaluronan on the target cells. Collectively, these results suggest that Metastatin is an effective antitumor agent that exhibits antiangiogenic activity.

INTRODUCTION

A potential therapeutic target on angiogenic endothelial cells is hyaluronan, a large negatively charged glycosaminoglycan that plays a role in the formation of new blood vessels (1). Particularly high concentrations of hyaluronan are associated with endothelial cells at the growing tips or sprouts of newly forming capillaries (2, 3). Similarly, when cultured endothelial cells are stimulated to proliferate by cytokines, their synthesis of hyaluronan is significantly increased (4). Interestingly, this stimulation is restricted to endothelial cells derived from the small blood vessels and is not seen in endothelial cells derived from larger ones (4). In the case of mature blood vessels, hyaluronan is present in perivascular regions and in the junctions between the endothelial cells (5, 6). Earlier studies have shown that exogenously applied hyaluronan has different effects on angiogenesis depending on its size, with macromolecular hyaluronan inhibiting vascularization in chicken embryos, and oligosaccharide fragments of hyaluronan stimulating vascularization in the chorioallantoic membrane (7–9). Thus, hyaluronan appears to be specifically associated with the endothelial cells of newly forming blood vessels and can influence their behavior.

In addition to hyaluronan, endothelial cells involved in neovascularization also express CD44 and other cell surface receptors for hyaluronan (10–12). In particular, endothelial cells associated with tumors express large amounts of CD44 (11). In previous studies, we have shown that CD44 allows cells to bind hyaluronan so that it can be internalized into endosomal compartments, where the hyaluronan is degraded by the action of acid hydrolases (13, 14). Thus, the expression of CD44 by endothelial cells allows them to bind and internalize hyaluronan as well as any associated proteins. The fact that both hyaluronan and CD44 are up-regulated in endothelial cells involved in neovascularization suggests that the turnover of hyaluronan by these cells is much greater than that by cells lining mature blood vessels.

The increased turnover of hyaluronan in tumor-associated endothelial cells suggested a possible mechanism to specifically target these cells. Our initial idea was to use a hyaluronan-binding complex isolated from cartilage to deliver chemotherapeutic agents specifically to these endothelial cells. Purified by affinity chromatography, this hyaluronan-binding complex consists of tryptic fragments of the link protein and aggrecan core protein (5, 15, 16). We intended to couple the hyaluronan-binding complex to a chemotherapeutic agent such as methotrexate and use this derivative to attack endothelial cells. We hoped that this derivative would bind to the hyaluronan on the endothelial cells and then be internalized into lysosomes. where the methotrexate would be released by the action of acid hydrolyses. Surprisingly, however, in the course of these experiments, we found that the hyaluronan-binding complex by itself (*i.e.*, in the absence of a chemotherapeutic agent) inhibited angiogenic activity. Functionally, we termed the hyaluronan-binding complex, which inhibits tumor growth, Metastatin.

In the present study, we demonstrate that Metastatin has a number of intriguing biological activities, including inhibition of endothelial cell proliferation and migration, inhibition of angiogenesis, and suppression of tumor cell growth in chicken embryos and pulmonary metastasis in mice. These effects are blocked by preincubating Metastatin with hyaluronan, suggesting that the activity of Metastatin depends on its ability to bind hyaluronan on the target cells.

MATERIALS AND METHODS

Preparation of Metastatin. The hyaluronan-binding complex was prepared by a modified version of the method originally described by Tengblad (15, 16). Briefly, bovine nasal cartilage (Pel-Freez, Rogers, AR) was shredded with a Sure-Form blade (Stanley), extracted overnight with 4 M guanidine-HCl and 0.5 M sodium acetate (pH 5.8), and dialyzed against distilled water to which 10× PBS was added to a final concentration of 1× PBS (pH 7.4). The protein concentration was measured, and for each 375 mg of protein. 1 mg of trypsin (type III; Sigma, St. Louis, MO) was added. After digestion for 2 h at 37°C. the reaction was terminated by the addition of 2 mg of soybean trypsin inhibitor (Sigma) for each milligram of trypsin. The digest was dialyzed against 4 M guanidine-HCl and 0.5 M acetate (pH 5.8), mixed with hyaluronan coupled to Sepharose, and then dialyzed against a 10-fold volume of distilled water. The hyaluronan-Sepharose beads were placed into a chromatography column and washed with 1.0 M NaCl. followed by a gradient of 1.0–3.0 M NaCl. Metastatin was eluted from the hyaluronan affinity column with 4 M guanidine-HCl and 0.5 M sodium acetate (pH 5.8), dialyzed against saline, and sterilized by passage through a 0.2-μm-pore filter. For SDS-PAGE analysis, the purified preparation was loaded onto a 10% BisTris nonreducing gel (Novex, Inc.) and subsequently stained with Coomassie Blue. To identify the
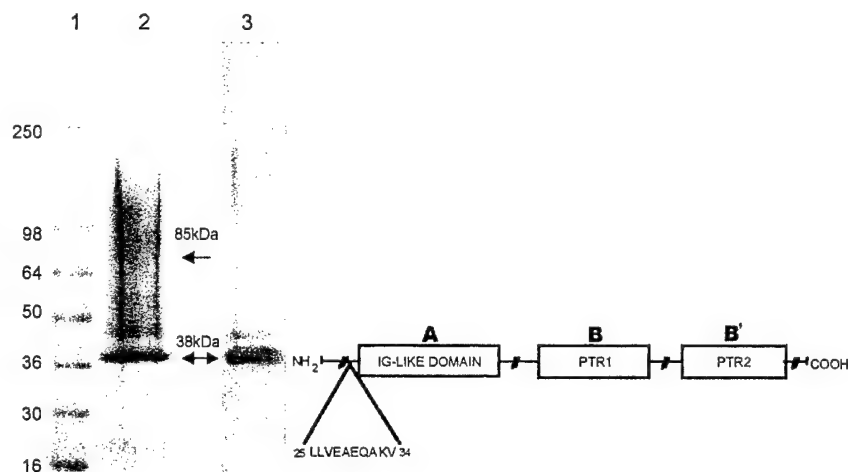
Fig. 1. SDS-PAGE and NH$_2$-terminal analysis of Metastatin. *Lane 1*, molecular mass markers; *Lane 2*, Metastatin stained with Coomassie blue; *Lane 3*, Western blot of Metastatin immunostained with an antibody against the link protein. The fragment of aggrecan migrated as a diffuse band at ~85 kDa, whereas the truncated link protein was at 38 kDa. NH$_2$-terminal sequence analysis of the 38-kDa band indicated that the first 24 amino acids of the link protein have been cleaved and is indicated on the schematic diagram.

link protein by Western blotting, the proteins on the gel were transferred to a sheet of nitrocellulose and immunostained with the 9/30/8-A-4 monoclonal antibody. (The monoclonal antibody, developed by Dr. B. Caterson, was obtained from the Developmental Studies Hybridoma Bank under the auspices of the NICHD and maintained by the University of Iowa, Department of Biological Sciences, Iowa City, IA 52242.) This identity was further confirmed by NH$_2$-terminal sequencing (Fig. 1). In tests of the biological activity of Metastatin, controls consisted of Metastatin mixed with an excess mass of hyaluronan (Lifecore, Chaska, MN) or a heat-inactivated preparation made by placing it in a boiling water bath for 30 min.

Endothelial and Tumor Cell Lines. HUVECs[4] were obtained from the Tumor Bank of the Lombardi Cancer Center (Georgetown University, Washington, DC). ABAEs were kindly provided by Dr. Luyuan Li (Lombardi Cancer Center), and BRECs were provided by Dr. Rosemary Higgins (Pediatrics, Georgetown University). These endothelial cells were cultured in 90% DMEM, 10% fetal bovine serum, and 10 ng/ml bFGF. The B16BL6 melanoma tumor line was obtained from the National Cancer Institute Central Repository (Frederick, MD), TSU cells were obtained from the American Type Culture Collection (Rockville, MD), and Lewis lung carcinoma cells were kindly supplied by Dr. Michael O'Reilly (Children's Hospital, Boston, MA). The tumor cells were grown in 90% DMEM, 10% fetal bovine serum, and 2 mM L-glutamine. For the mouse metastasis assays, cells were generally used between passages 6 and 18.

Mice. Specific pathogen-free, male, 6–8-week-old C57Bl/6 mice were obtained from The Jackson Laboratory (Bar Harbor, ME). Animals were cared for and treated in accordance with the procedures outlined in the Guide for the Care and Use of Laboratory Animals (NIH Publication No. 86-23). Animals were housed in a pathogen-free environment and provided with sterilized animal chow (Harlan Sprague Dawley, Indianapolis, IN) and water *ad libitum*.

Mouse Metastasis Model System. For the experimental melanoma model, mice were inoculated i.v. in the lateral tail vein with B16Bl6 cells (5×10^4 cells/animal) on day 0. Treatment was initiated on day 3 with 5 (0.2 mg/kg), 15 (0.6 mg/kg), and 49 μg (2 mg/kg) of Metastatin and continued daily until animals were sacrificed on day 14. After euthanasia, the lungs were removed, and surface metastatic lesions were enumerated under a dissecting microscope.

Mice were also inoculated with Lewis lung carcinoma cells, which aggressively form pulmonary metastases. Mice were injected i.v. in the lateral tail vein with 2.5×10^5 cells/animal (day 0), and beginning on day 3, the Metastatin was administered by daily i.p. injections of 15 (0.6 mg/kg) and 49 μg (2 mg/kg) or by three i.v. injections of 100 μg (4 mg/kg) on days 1, 3, and 5. Animals were euthanized, and their lungs were removed and weighed. To obtain the lung weight gain, the average lung weight of nontreated mice (0.2 g) was subtracted from that of the treated animals.

The number of pulmonary metastases and lung weight gains were reported as mean $\pm$ SD, and the differences were compared using Student's *t* test. The

groups were considered to be different when the probability (*P*) value was <0.05.

Chicken Chorioallantoic Membrane Assays. To measure angiogenesis, a chick chorioallantoic membrane assay was performed using a modification of the methods of Brooks *et al.* (17). For this, holes were drilled in the tops of 10-day-old chicken eggs to expose the chorioallantoic membranes, and filter discs (0.5 cm in diameter) containing 20 ng of human recombinant VEGF [20 μl (1 μg/ml); Pepro, Rocky Hill, NJ] were placed on the surface of each chorioallantoic membrane (day 0). The holes were covered with parafilm, and the eggs were incubated at 37°C in a humidified atmosphere. One day later, the eggs were given injections (via a blood vessel in the chorioallantoic membrane using a 30-gauge needle) of the various substances [Metastatin (80 μg/egg) or controls consisting of PBS or heat-inactivated Metastatin]. Three days later (day 4), the chorioallantoic membranes and associated discs were cut out and immediately immersed in 3.7% formaldehyde. For computer-assisted image analysis, the discs were divided into quarters with fine wires, and the blood vessels in each quarter were digitally photographed and analyzed by an Optimas 5 program to calculate the vessel area and length normalized to the total area measured. The means and the SEs were calculated from all quadrants within each group, and the statistical significance was determined by Student's *t* test. Twelve or more eggs were used for each sample point.

For the growth of xenografts on the chorioallantoic membrane, holes were cut into the sides of 10-day-old eggs exposing the membrane (day 0), and then 1×10^6 B16BL6 or TSU cells were applied to the membranes. Two days later, the eggs were given i.v. injections of the various substances. On day 7, the tumor masses were fixed in formalin, dissected free from the normal membrane tissue, and weighed.

Cell Growth Assays. To determine the effects of Metastatin on cell growth, the cell lines were subcultured into 24-well dishes at a density of approximately 5×10^5 cells/well for the endothelial cell lines (HUVEC, ABAE, and BREC) and 5×10^4 cells/well for tumor cell lines (B16BL6, TSU, and Lewis lung carcinoma). For the dose-response experiments, the medium was changed every other day, and at the end of 6 days, the cells were released with 0.5 mM EDTA in PBS, and the cell number was determined with a Coulter counter (Hialeah, FL).

ELISA Assay for Hyaluronan. Cells were grown to confluence in 24-well dishes, and the conditioned medium was collected, incubated with a biotinylated version of the Metastatin (16), and then transferred to plates precoated with hyaluronan (umbilical cord; Sigma). The hyaluronan present in the conditioned medium interacts with the biotinylated Metastatin so that less of it will be left to bind to hyaluronan attached to the plate. At the end of the incubation, the plates were washed, and the amount of biotinylated Metastatin remaining attached was determined by incubating the plates with streptavidin coupled to peroxidase (Kirkegard & Perry, Gaithersburg, MD) followed by a soluble substrate for peroxidase. The amount of hyaluronan in the conditioned medium was calculated by comparison with a standard curve with known amounts of hyaluronan (16).

---

[4] The abbreviations used are: HUVEC, human umbilical vein endothelial cell; ABAE, adult bovine aorta endothelial cell; BREC, bovine retinal endothelial cell; VEGF, vascular endothelial growth factor; bFGF, basic fibroblast growth factor.

Wound Migration Assay. A suspension of HUVECs (5×10^5 cells in 5 ml of 98% M199 and 2% fetal bovine serum) was added to 60-mm tissue culture plates that had been precoated with gelatin (2 ml of 1.5% gelatin in PBS, 37°C, overnight) and allowed to grow for 3 days to confluence. An artificial "L"-shaped wound was generated in the confluent monolayer with a sterile razor blade by moving the blade down and across the plate. Plates were then washed with PBS, and 2 ml of PBS were added to each plate along with 2 ml of sample in M199 and 2% fetal bovine serum in the presence and absence of 5 ng/ml bFGF. After an overnight incubation, the plates were treated with Diff-Quik for 2 min to fix and stain the cells. The number of cells that migrated were counted under ×200 magnification using a 10-mm micrometer over a 1 cm distance along the wound edge. Ten fields for each plate were counted, and an average for the duplicate was calculated.

RESULTS

Characterization of Metastatin. Metastatin was isolated from bovine nasal cartilage by affinity chromatography on hyaluronan-Sepharose. As shown in Fig. 1, Metastatin consisted of two molecular factions as determined by SDS-PAGE, a sharp band at 38 kDa that corresponds to the link protein, and a diffuse band at approximately 85 kDa that represents a tryptic fragment of the aggrecan core protein (5, 15, 16). The diffuse nature of this latter fraction is probably due to variations in the degree of glycosylation and glycosaminoglycan content. The identity of the link protein was verified by immunoblotting with a specific monoclonal antibody against this protein (Fig. 1). In addition, NH_2-terminal sequence analysis of the 38-kDa band revealed that the purified protein was missing the first 24 amino acids. Previous studies have shown that this complex binds to hyaluronan with high affinity and specificity (5, 16). Indeed, a biotinylated version of the preparation has been widely used as a histochemical stain to localize hyaluronan in tissue sections (5, 16).

Because cartilage is known to contain various protease inhibitors, which may contribute to its antitumor properties (18), we wanted to determine whether Metastatin possessed such attributes. For this reason, we used a chromogenic assay (Diapharma Group, Inc., West Chester, OH) to assess the effect of Metastatin on the following enzymes: (*a*) trypsin; (*b*) chymotrypsin; (*c*) plasmin; and (*d*) elastase. At concentrations as high as 100 μg/ml, Metastatin did not inhibit the activity of any of the enzymes tested (data not shown).

Effect of Metastatin on Metastatic Tumors. In initial experiments, we found that Metastatin was effective at inhibiting pulmonary metastases of B16BL6 cells. When mice were given daily i.p. injections of Metastatin 3 days after tumor inoculation, lung metastases were strikingly reduced (Fig. 2A). Fig. 2B shows that the number of surface lung metastases (>0.5 mm) in the mice treated with 15 and 49 μg Metastatin/day were reduced by more than 80%. The dose-response curve shown in Fig. 2C was constructed from two independent experiments and shows that Metastatin decreased the number of metastatic colonies in a dose-dependent manner with an ED_{50} of approximately 10 μg (0.4 mg/kg). Significantly, when Metastatin preparations were premixed with macromolecular hyaluronan, the antimetastatic activity was blocked, and the mean number of surface pulmonary metastases was comparable to that seen in control mice (Fig. 2B). This suggests that the ability of Metastatin to bind hyaluronan is required for its anti-tumor activity.

Similar results were obtained with the Lewis Lung carcinoma cell line, which is a more aggressive mouse tumor model. As shown in Fig. 3, *A* and *B*, Metastatin inhibited pulmonary metastasis of Lewis lung carcinoma cells in a dose-related fashion, as reflected in the weight gain of the lungs. Furthermore, Metastatin was effective when given by two different routes, i.p. and i.v. (Fig. 3, *B* and *C*).
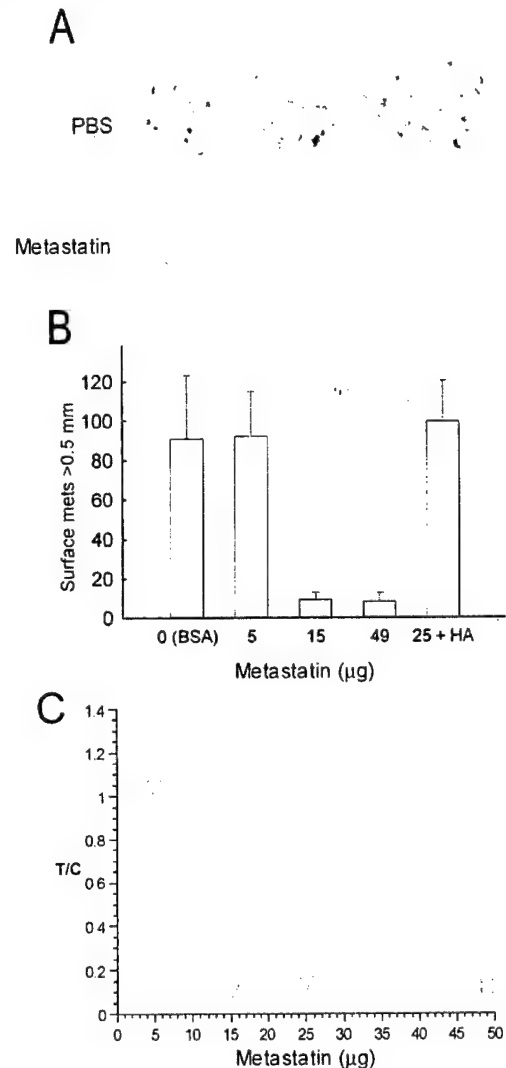
Fig. 2. Effect of Metastatin on B16BL6 melanoma metastasis. B16BL6 melanoma cells were injected into the tail veins of C57Bl/6 mice, and 3 days later, the mice were injected i.p. with increasing doses of Metastatin. After 14 days, the lungs were removed, and surface pulmonary metastases were counted. *A*, the lungs from control animals had a greater number of metastases than those from the Metastatin (49 μg)-treated animals. *B*, the number of pulmonary metastases larger than 0.5 mm is plotted against the concentration of Metastatin injected. Metastatin inhibits the number of metastases, and the addition of hyaluronan to Metastatin blocked its inhibitory activity. The values shown are the mean of at least five mice/group; *bars*, SD. *C*, this dose-response curve was derived from two independent experiments (*n* = 5 for each point) and shows the ratio of pulmonary metastasis in the test and control animals (*T/C*) as a function of the Metastatin dose.

Effect of Metastatin on *in Vitro* Cell Proliferation and Migration. In the next series of experiments, we wanted to determine whether Metastatin has any effect on the growth of either endothelial or tumor cells in tissue culture. For these experiments, the cells were grown in the presence of varying concentrations of Metastatin for 6 days, and then the final cell numbers were determined. Metastatin inhibited the proliferation of the endothelial cell lines HUVEC, ABAE, and BREC (Fig. 4A) and two of the tumor cell lines (B16BL6 and Lewis lung carcinoma cells) but had no effect on the TSU cells (Fig. 4B). Similar results were obtained when proliferation was monitored by incorporation of bromodeoxyuridine (data not shown). It is important to note that the growth inhibition of B16BL6 cells was partially blocked when the preparation of Metastatin was premixed with an excess of hyaluronan (Fig. 4B).

One possible explanation for the lack of TSU cell sensitivity to
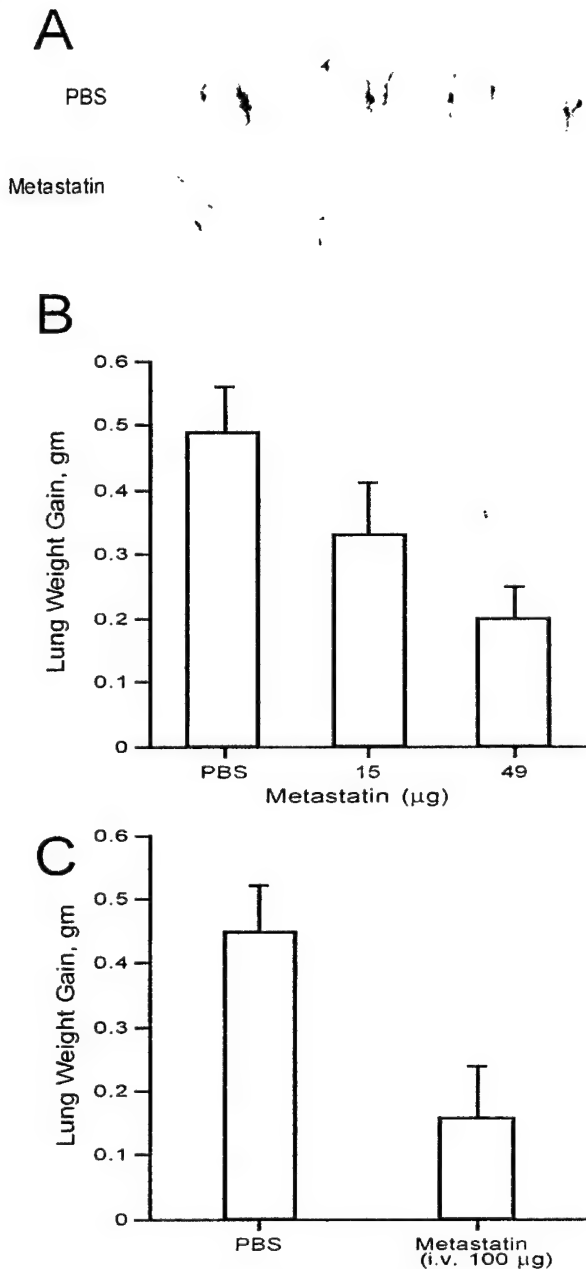
A

PBS

Metastatin

B

C

Fig. 3. Inhibition of pulmonary metastasis of Lewis lung carcinoma cells. Lewis lung carcinoma cells were injected into the tail veins of C57Bl/6 mice, and 3 days later, mice were treated with PBS or Metastatin. Once the treatment was stopped, animals were euthanized, and lungs were removed and weighed. *A*, shows representative lungs from control and treated animals and illustrates that Metastatin lowers the tumor burden. *B*, Metastatin injected i.p. daily beginning on day 4 decreased the relative lung weights in a dose-dependent fashion. *C*, the weight of the lungs in animals was also decreased when Metastatin was administered by three separate i.v. injections (100 μg/injection on days 1, 3, and 5). The values shown are the mean of at least five mice/group; *bars*, SD.

Metastatin could be the amount of hyaluronan that they secrete because it has an inhibitory effect. To test this possibility, conditioned media from confluent cultures of the different cell lines were collected and analyzed for hyaluronan by a modified ELISA. TSU cells were found to secrete significantly larger amounts of hyaluronan into the medium than the other cell lines (7 μg/ml *versus* <0.5 μg/ml, respectively). Indeed, this level of hyaluronan would be sufficient to block the effects of added Metastatin.

We also examined the effects of Metastatin on the migration of endothelial cells, another important factor in the process of angiogenesis (19). In this assay, we examined the effect of Metastatin on the

migration of HUVECs using the wound migration assay. Fig. 5 shows that at a concentration of 10 μg/ml, Metastatin inhibited the migration of HUVECs by 50% as compared with controls treated with bFGF alone. Again, similar results were obtained when migration was monitored using Nucleopore filters (data not shown).

Effect of Metastatin on VEGF-induced Angiogenesis. The fact that Metastatin could inhibit both the growth and migration of endothelial cells *in vitro* suggested that it might also be able to block angiogenesis *in vivo*. To test this possibility, we examined the effect
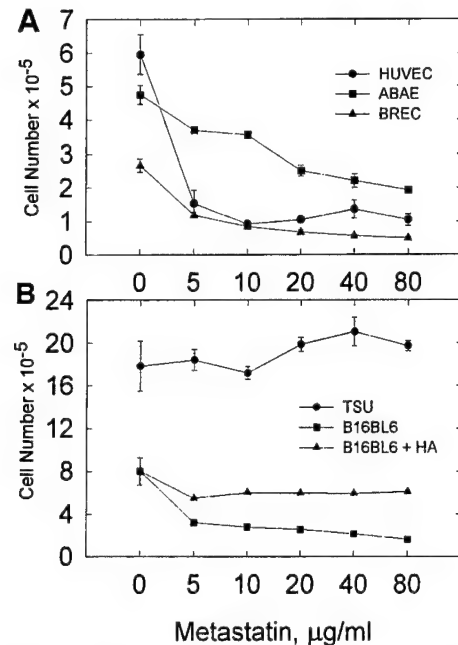

Fig. 4. The effects of varying concentrations of Metastatin on the growth of cultured cells. The cell lines were cultured in 24-well dishes in complete medium containing the indicated amounts of Metastatin, with medium changes ever other day. After 6 days, the cells were harvested with a solution of EDTA in PBS, and the cell numbers were determined with a Coulter counter. *A*, a dose-response curve is shown for the effects of Metastatin on the growth of the endothelial cell lines HUVEC, ABAE, and BREC. In each case, the growth of the cells was inhibited by Metastatin. *B*, a dose-response plot is shown for the tumor cell lines B16BL6 and TSU. Whereas Metastatin inhibited the growth of the B16BL6 cells, it had little or no effect on the TSU cells. The addition of an equal mass of hyaluronan to the Metastatin significantly reduced its effect on the proliferation of B16BL6 cells.

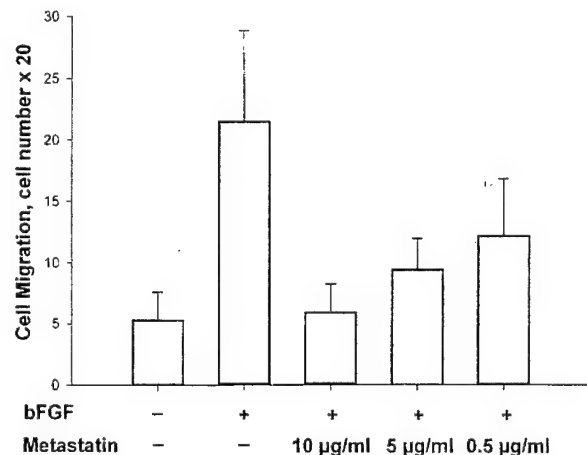| bFGF | − | + | + | + | + |
| Metastatin | − | − | 10 µg/ml | 5 µg/ml | 0.5 µg/ml |

Fig. 5. Dose-dependent inhibitory effect of Metastatin on the migration of endothelial cells. HUVECs were grown to confluence on gelatin-coated culture plates, wounded with a sterile razor blade, and induced to migrate with bFGF in the presence of varying amounts of Metastatin. The number of cells that migrated were enumerated using a micrometer and microscope at ×200 magnification.
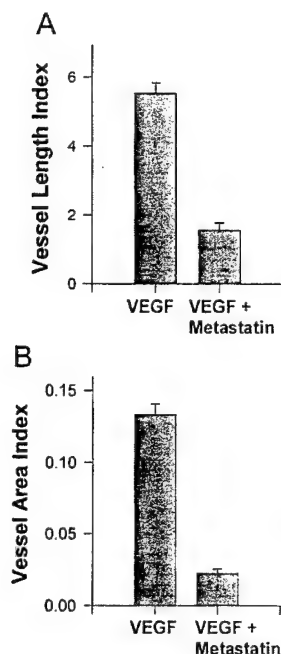
A

B

Fig. 6. Effect of Metastatin on VEGF-induced angiogenesis. The top of air sacs of 10-day-old chicken eggs were opened, exposing the chorioallantoic membranes, and filter discs containing 20 ng of VEGF were applied. The treated group was then injected i.v. with Metastatin (80 μg/egg), and the control group did not receive injections. The chorioallantoic membranes and associated discs were cut out on day 3 and analyzed by computer-assisted image analysis as described in "Materials and Methods". Metastatin had a significant inhibitory effect on both the (A) vessel length index and (B) vessel area index.

of Metastatin on angiogenesis induced in the chick chorioallantoic membrane. In this assay, filter papers containing recombinant human VEGF were placed on the chorioallantoic membrane of 10-day-old eggs, which were then given a single i.v. injection of the Metastatin or control preparations. Three days later, the extent of vascularization in the region of the filters was determined by computer-assisted image analysis. As shown in Fig. 6, treatment with Metastatin reduced both the length and area of vessels as compared with the control group, suggesting that Metastatin does indeed have the ability to block VEGF-induced angiogenesis.

Inhibition of Tumor Growth on the Chorioallantoic Membrane. To further explore the antitumor activity of Metastatin, we examined its effect on the growth of B16BL6 and TSU cells on the chicken chorioallantoic membrane. Tumor cells were applied to the chorioallantoic membranes of 10-day-old chicken embryos and allowed to grow for 1 week. Pilot experiments revealed that after inoculation with 10^6 cells, the take rate was almost 100% and resulted in xenografts with weights from 50–150 mg in 7 days. However, when the inoculated eggs were given a single i.v. injection of the Metastatin, the growth of the B16BL6 and TSU xenografts was greatly inhibited (Fig. 7). Again, this inhibitory effect was abolished if the preparation of Metastatin was heat inactivated or preincubated with its ligand, hyaluronan (Fig. 7B). It is important to note that Metastatin did not appear to adversely affect the development of the chicken embryos.

DISCUSSION

In this study we report that Metastatin, a cartilage-derived hyaluronan-binding complex consisting of proteolytic fragments of bovine link protein and aggrecan, is able to block the growth and metastasis of tumor cells under the following conditions: (a) a single i.v. injection of Metastatin into the chorioallantoic membrane of chicken

embryos inhibited the growth of B16BL6 mouse melanoma cells and TSU human prostate cancer cells; (b) multiple i.p. injections of Metastatin prevented the experimental metastasis of B16BL6 and Lewis lung carcinoma cells to the lungs of mice; and (c) three i.v. injections of Metastatin were sufficient to inhibit the formation of Lewis lung carcinoma metastasis. In each case, Metastatin did not have an obvious detrimental effect on the host and was neutralized by complexing with soluble hyaluronan.

Metastatin is a member of a family of hyaluronan-binding proteins that also includes CD44, tumor necrosis factor-stimulated gene 6 (TSG-6), versican, neurocan, and brevican (20). Interestingly, Metastatin is similar to other factors that influence angiogenesis in that it is a fragment of a larger complex. For example, Angiostatin is a fragment of plasminogen, Endostatin represents a fragment of collagen XVIII, and serpin consists of a fragment of antithrombin (21–24). It is possible that the production of the peptide fragments is part of a feedback loop important in the down-regulation of angiogenesis.

In addition to Metastatin, a number of other antiangiogenic factors have been isolated from cartilage. Indeed, cartilage has been extensively studied as a source of molecules that could account for its avascular nature. Langer et al. (25) first reported a bovine cartilage fraction isolated by guanidine extraction and purified by trypsin affinity chromatography that inhibited tumor-induced vascular proliferation. In addition, Moses et al. (26) have recently isolated Troponin I from veal scapulae, which was shown to have antitumor and antiangiogenic properties. Lee and Langer (27) have described a guanidine-extracted factor from shark cartilage that inhibited angiogenesis and suppressed tumor vascularization. Similarly, Moses et al. (18) isolated a factor from cultures of scapular chondrocytes that inhibited angiogenesis in the chicken chorioallantoic membrane and appeared to be a protease inhibitor. However, it is likely that our preparation of Metastatin acts through a distinct mechanism because it has no detectable antiprotease activity and is inhibited by the addition of hyaluronan. It is tempting to speculate that Metastatin may contribute to the avascular nature of cartilage. Along these lines, we have previously found that hypertrophic chondrocytes produce large amounts of free hyaluronan, which may neutralize the effects of Metastatin in this region and thereby allow blood vessels to invade (28).

The results of this study suggest that Metastatin has antiangiogenic properties as demonstrated by its ability to block VEGF-induced formation of blood vessels in the chicken chorioallantoic membrane. The antiangiogenic effect of Metastatin was also consistent with our finding that it blocked both the proliferation and migration of cultured endothelial cells. Whereas Metastatin can directly attach tumor cells, we believe that most of its antitumor activity is due to its inhibition of angiogenesis because after its injection, the first cells that it would encounter are the endothelial cells, which would be exposed to the highest concentration. In addition, this antiangiogenic mechanism is suggested by the fact that Metastatin blocked the growth of TSU cells in vivo (i.e., on the chicken chorioallantoic membrane) but had little or no effect on their proliferation in vitro. In this particular case, it seems likely that Metastatin was acting indirectly on the TSU tumor cells by blocking angiogenesis.

In other cases, the antitumor activity of Metastatin may be due to the combined action of direct killing of the tumor cells and the inhibition of angiogenesis. Indeed, Metastatin does appear to partially inhibit the growth of B16BL6 in tissue culture, and it could presumably have a similar effect in vivo. Because many blood vessels that are associated with tumors are leaky (29), Metastatin may be able to escape the circulation to interact directly with the tumor cells and block their proliferation. Along these lines, a recent study by Maniotis et al. (30) has indicated that some tumors have the ability to form
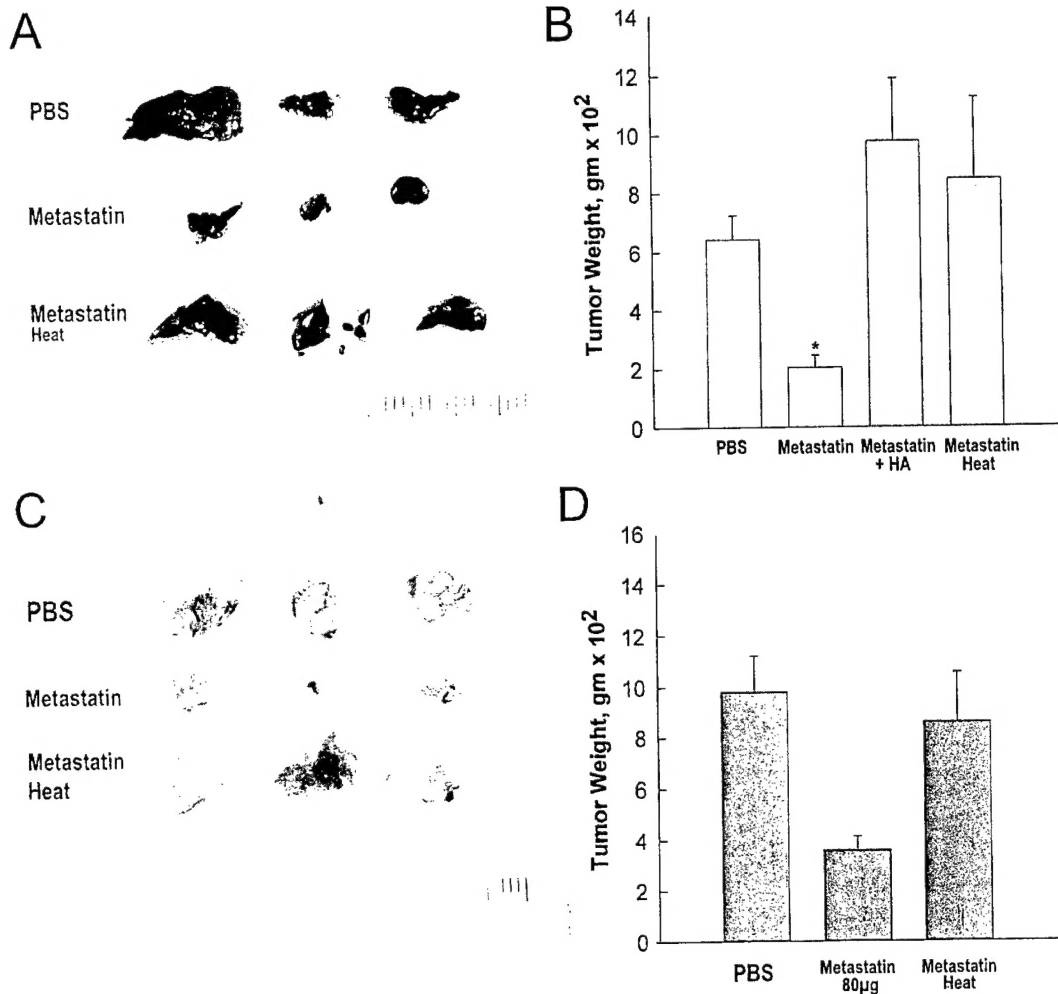
Fig. 7. Effect of Metastatin on the growth of tumor cells on the chicken chorioallantoic membrane. The top of the air sacs of 10-day-old chicken eggs were opened, exposing the chorioallantoic membrane, and pellets containing B16BL6 melanoma or TSU prostate tumor cells were placed on the membrane. On day 3, the embryos were given a single i.v. injection of PBS or Metastatin (80 μg). The tumors and associated chorioallantoic membranes were removed on day 6 and weighed. A and C, examples of the B16BL6 and TSU xenografts from eggs treated with PBS, Metastatin, or heat-denatured Metastatin. B and D, the weights of B16BL6 and TSU xenografts from eggs treated with Metastatin and control preparations are shown.

vasculature independent of endothelial cells. The tumor cells themselves appear to take on the characteristics of endothelial cells and are responsible for the formation of blood vessels. It is possible that such dual-acting tumor cells could also respond to Metastatin.

The biological effects of Metastatin appear to be closely linked to its ability to bind hyaluronan. If the preparation of Metastatin was premixed with hyaluronan, then this reversed its inhibitory effects on tumor growth in vivo and in vitro and its effects on the growth and migration of cultured endothelial cells. This indirectly suggests that Metastatin is binding to hyaluronan associated with the target cell. In the case of endothelial cells, particularly high levels of hyaluronan are localized to the tips of newly forming capillaries in the chicken chorioallantoic membrane and rabbit cornea (2, 3). A variety of other cell types show a similar relationship between proliferation and the production of hyaluronan (31–34). Whereas the hyaluronan present on proliferating tumor and endothelial cells could interact directly with Metastatin in the blood, the hyaluronan in other locations would not be exposed to high concentrations of the complex. Most normal cells would be protected by the fact that high concentrations of hyaluronan are present in connective tissues such as the dermis, lamina propria, and capsules (5, 35, 36), which would help to neutralize the Metastatin that diffused into these regions. It is important to note that under normal physiological conditions, hyaluronan in the

blood is maintained at low levels by the liver and lymphatic system (37, 38). Thus, the circulating Metastatin should retain its hyaluronan binding activity.

Cell surface hyaluronan may serve as a target for other inhibitors of angiogenesis and tumor growth. For example, Endostatin, a ~20-kDa fragment of the COOH-terminal of collagen XVIII that inhibits angiogenesis (21, 22), may also be able to bind hyaluronan, as suggested by the presence of specific structural motifs (39). Secondly, a soluble, recombinant version of immunoglobulin fused with CD44 that binds to hyaluronan can inhibit the growth of human lymphoma cells that express CD44 in nude mice (40, 41). TSG-6, which is secreted by a variety of cells after stimulation with inflammatory cytokines, is able to both bind hyaluronan and block tumor cell growth (42). In each of these cases, these factors may be interacting with hyaluronan on the surfaces of target cells to exert their effects on angiogenesis and tumor growth.

In preliminary studies, we have found that Metastatin induces apoptosis in the target cells. However, at present, the mechanism by which Metastatin is able to do this is unclear. One possibility is that after Metastatin has bound to hyaluronan on the cell surface, it is taken up by the cells into lysosomes, where it is broken down into smaller fragments that enter the cytoplasm and induce apoptosis, perhaps by interacting with the mitochondrial membrane. Alternatively, Metasta-

tin could be interacting directly with the plasma membrane of the target cells, causing damage that in turn induces the apoptotic cascade. Clearly, future experiments will be directed toward elucidating the mechanism by which Metastatin induces apoptosis in the target cells.

In conclusion, we have found that Metastatin is able to block tumor growth in two model systems, and this effect depends on its ability to bind hyaluronan. Metastatin appears to target both tumor cells and endothelial cells that are involved in neovascularization. We postulate that during angiogenesis, the endothelial cells up-regulate their synthesis of hyaluronan, which then serves as a target for the injected Metastatin. Thus, Metastatin may represent a new type of antitumor agent, which targets cell surface hyaluronan.

ACKNOWLEDGMENTS

REFERENCES

1. Rooney, P., Kumar, S., Ponting, J., and Wang. M. The role of hyaluronan in tumor neovascularization. Int. J. Cancer, 60: 632–636, 1995.
2. Ausprunk, D. H., Boudreau, C. L., and Nelson, D. A. Proteoglycans in the microvasculature. II. Histochemical localization in proliferating capillaries of the rabbit cornea. Am. J. Pathol., 103: 367–375, 1981.
3. Ausprunk, D. H. Distribution of hyaluronic acid and sulfated glycosaminoglycans during blood vessel development in the chick chorioallantoic membrane. Am. J. Pathol., 177: 313–331, 1986.
4. Mohamadzadeh, M., DeGrendele, H., Arizpe, H., Estess, P., and Siegelman, M. Proinflammatory stimuli regulate endothelial hyaluronan expression and CD44/HA-dependent primary adhesion. J. Clin. Investig., 101: 97–108, 1998.
5. Green, S. J., Tarone, G., and Underhill, C. B. The distribution of hyaluronate and hyaluronate receptors in the adult lungs. J. Cell Sci., 89: 145–156, 1988.
6. Eggli, P. S., and Graber, W. Association of hyaluronan with rat vascular endothelial and smooth muscle cells. J. Histochem. Cytochem., 43: 689–697, 1995.
7. Feinberg, R. N., and Beebe, D. C. Hyaluronate in vasculogenesis. Science (Washington DC), 220: 1177–1179, 1983.
8. West, D. C., Hampson, I. N., and Kumar, S. S. Angiogenesis induced by degradation products of hyaluronic acid. Science (Washington DC), 228: 1324–1326, 1985.
9. Deed, R. P., Rooney, P. L., Kumar, J. D., Norton, J., Smith, A., Freemont, J., and Kumar, S. Early-response gene signaling is induced by angiogenic oligosaccharides of hyaluronan in endothelial cells. Inhibition by non-angiogenic, high-molecular-weight hyaluronan. Int. J. Cancer, 71: 251–256, 1997.
10. Banerjee, S. D., and Toole, B. P. Hyaluronan-binding protein in endothelial cell morphogenesis. J. Cell Biol., 119: 643–652, 1992.
11. Griffioen, A. W., Goenen, M. J. H., Damen, C. A., Hellwig, S. M. M., van Weering, D. H. J., Vooys, W., Blijham, G. H., and Groenewegen, G. CD44 is involved in tumor angiogenesis; an activation antigen on human endothelial cells. Blood, 90: 1150–1159, 1997.
12. Banerji, S., Ni, J. Wang, S-X., Clasper, S., Su, J., Tammi, R., Jones, M., and Jackson, D. G. LYVE-1, a new homologue of the CD44 glycoprotein, is a lymph-specific receptor for hyaluronan. J. Cell Biol., 144: 789–801, 1999.
13. Culty, M., Nguyen, H. A., and Underhill, C. B. The hyaluronan receptor (CD44) participates in the uptake and degradation of hyaluronan. J. Cell Biol., 116: 1055–1062, 1992.
14. Culty, M., Shizari, M., Thompson, E. W., and Underhill, C. B. Binding and degradation of hyaluronan by human breast cancer cell lines expressing different forms of CD44: correlation with invasive potential. J. Cell. Physiol., 160: 275–286, 1994.
15. Tengblad, A. Affinity chromatography on immobilized hyaluronate and its applications to the isolation of hyaluronate binding proteins from cartilage. Biochim. Biophys. Acta., 578: 281–289, 1979.
16. Underhill, C. B., and Zhang, L. Analysis of hyaluronan using biotinylated hyaluronan-binding proteins. Methods Mol. Biol., 137: 441–447, 1999.
17. Brooks, P. C., Silletti, S., von Schalscha, T. L., Friedlander, M., and Cheresh, D. A. Disruption of angiogenesis by PEX, a noncatalytic metalloproteinase fragment with integrin binding activity. Cell, 92: 391–400, 1998.
18. Moses, M. A., Sudhalter, J., and Langer, R. Isolation and characterization of an inhibitor of neovascularization from scapular chondrocytes. J. Cell Biol., 119: 473–482, 1992.
19. Ausprunk, D. H., and Folkman, J. Migration and proliferation of endothelial cells in preformed and newly formed blood vessels during tumor angiogenesis. Microvasc. Res., 14: 53–65, 1977.
20. Neame, P. J., and Barry, F. P. The link protein. Experientia (Basel), 49: 393–402, 1993.
21. Folkman, J., and Shing, Y. Angiogenesis. J. Biol. Chem., 267: 10931–10934, 1992.
22. O'Reilly, M. S., Boehm, T., Shing, Y., Fukai, N., Vasios, G., Lane, W. S., Flynn, E., Birkhead, J. R., Olsen, B. R., and Folkman, J. Endostatin. An endogenous inhibitor of angiogenesis and tumor growth. Cell, 88: 277–285, 1997.
23. O'Reilly, M. S., Holmgren, L., Shing, Y., Chen, C., Rosenthal, R. A., Moses, M., Lane, W. S., Cao, Y., Sage, E. H., and Folkman, J. Angiostatin. A novel angiogenesis inhibitor that mediates the suppression of metastases by a Lewis lung carcinoma. Cell, 79: 315–328, 1994.
24. O'Reilly, M. S., Pirie-Sheperd, S., Lane, W. S., and Folkman, J. Antiangiogenic activity of the cleaved conformation of the serpin antithrombin. Science (Washington DC), 285: 1926–1928, 1999.
25. Langer, R., Brem, H., Falterman, K., Klein, M., and Folkman, J. Isolations of a cartilage factor that inhibits tumor neovascularization. Science (Washington DC), 193: 70–72, 1976.
26. Moses, M. A., Wiederschain, D., Wu, I., Fernandez, C. A., Ghazizadeh, V., Lane, W. S., Flynn, E., Sytkowski, A., Tao, T., and Langer, R. Troponin I is present in human cartilage and inhibits angiogenesis. Proc. Natl. Acad. Sci. USA, 96: 2645–2650, 1999.
27. Lee, A., and Langer, R. L. Shark cartilage contains inhibitors of tumor angiogenesis. Science (Washington DC), 221: 1185–1187, 1983.
28. Pavasant, P., Shizari, M., and Underhill, C. B. Distribution of hyaluronan in the epiphysial growth plate: Turnover by CD44 expressing osteoprogenitor cells. J. Cell Sci., 107: 2669–2677, 1994.
29. Dvorak, H. F., Nagy, J. A., Dvorak, J. T., and Dvorak, A. M. Identification and characterization of the blood vessels of solid tumors that are leaky to circulating macromolecules. Am. J. Pathol., 133: 95–109, 1988.
30. Maniotis, A. J., Folberg, R., Hess, A., Seftor, E. A., Gardner, L. M. G., Pe'er, J., Trent, J. M., Meltzer, P. S., and Hendirx, M. J. Vascular channel formation by human melanoma cells in vivo and in vitro: vasculogenic mimicry. Am. J. Pathol., 155: 739–752, 1999.
31. Main, N. Analysis of cell-growth-phase-related variation in hyaluronate synthase activity of isolated plasma-membrane fractions of cultured human skin fibroblasts. Biochem. J., 237: 333–342, 1986.
32. Tomida, M., Koyama, H., and Ono, T. Induction of hyaluronic acid synthetase activity in rat fibroblasts by medium change of confluent cultures. J. Cell. Physiol., 86: 121–130, 1975.
33. Hronowski, L., and Anastassiades, T. P. The effect of cell density on net rates of glycosaminoglycan synthesis and secretion by cultured rat fibroblasts. J. Biol. Chem., 255: 10091–10099, 1980.
34. Matuoka, K., Namba, M., and Mitsui, Y. Hyaluronate synthetase inhibition by normal and transformed human fibroblasts during growth reduction. J. Cell Biol., 104: 1105–1115, 1987.
35. Alho, A. M., and Underhill, C. B. The hyaluronate receptor is preferentially expressed on proliferating epithelial cells. J. Cell Biol., 108: 1557–1565, 1989.
36. Underhill, C. B. The interaction of hyaluronate with the cell surface: the hyaluronate receptor and the core protein. CIBA Found. Symp., 143: 87–106, 1989.
37. Fraser, J. R. E., Appelgren, L. E., and Laurent, T. C. Tissue uptake of circulating hyaluronic acid. Cell Tissue Res., 233: 285–293, 1983.
38. Laurent, T. C., and Fraser, J. R. E. The properties and turnover of hyaluronan. Laurent, removal of HA from the blood. CIBA Found. Symp., 124: 9–29, 1986.
39. Hobenester, E., Sasaki, T., Olsen, B. R., and Timpl, R. Crystal structure of the angiogenesis inhibitor endostatin at 1.5 A resolution. EMBO J., 17: 1656–1664, 1998.
40. Sy, M-S., Guo, Y. J., and Stamenkovic, I. Inhibition of tumor growth in vivo with a soluble CD44-immunoglobulin fusion protein. J. Exp. Med., 176: 623–627, 1992.
41. Yu, Q., Toole, B. P., and Stamenkov, I. Induction of apoptosis of metastatic mammary carcinoma cells in vivo by disruption of tumor cell surface CD44 function. J. Exp. Med., 186: 1985–1996, 1997.
42. Wisniewski, H. G., Hua, J-C., Poppers, D. M., Naime, D., Vilcek, J., and Cronstein, B. N. TSG-6, a glycoprotein associated with arthritis, and its ligand hyaluronan exert opposite effects in a murine model of inflammation. J. Immunol., 156: 1609–1615, 1996.

#382 Hyaluronan Binding Motifs Inhibit Tumor Growth. Ningfei Liu, Xue-Ming Xu, Charles B. Underhill, Yixin Chen, Jinguo Chen Chen, Feng Gao, Zeqiu Han, and Lurong Zhang. *Lombardi Cancer Center, Washington, DC.*

Cartilage, enriched with hyaluronan (HA) binding proteins, has been proved to have anti-tumor effect in some clinical trails. To explore if HA binding motif is responsible for anti-tumor effect, a 39 peptide (called P4) containing three HA binding motifs was linked with NGR homing motif on its N-terminal and tested for anti-tumor function. The synthetic P4 could bind to 3H-HA with high capacity. When TSU prostate cancer cells, MDA-435 breast cancer cells and/or endothelial cells were treated with 50-100 ug/ml of P4, their growth was strongly inhibited in either anchorage-dependent or anchorage-independent conditions. This inhibitory effect was abolished by pre-incubation of P4 with HA, indicating the activated HA binding sites are crucial for the effect. In addition, when 100 ug of P4 was i.v. injected into CAM of chicken embryo bearing with tumors formed by B16 melanoma or MDA-435 cells, the tumor sizes were greatly reduced compared to the control. To see the potential of P4 for gene therapy, the amino acid sequence of P4 was back-translated into nucleotide sequence. The cDNA coding for P4 was inserted into the pSecTag2 vector with a signal peptide and transfected into TSU and MDA-435 cells. The growth of tumors formed by cells expressing P4 was inhibited compared to the control cells in both CAM and nude mice models. The angiogenesis in P4 tumors was reduced as determined by endothelial cells staining. Furthermore, the apoptotic indexes (Annexin$-\pi$ staining and nuclear fragmentation) were increased in both tumor cells and endothelial cells upon the treatment of P4, indicating that the inducing of apoptosis is one of action mechanisms by which P4 exerts anti-tumor effect. The involvement of lysosome and mitochondria in the P4 induced cell death has been investigated.

#383 Targeted Peptide of Human Brain Hyaluronan Binding Protein Inhibits Tumor Growth. Xueming Xu, Yixin Chen, Ningfei Liu, Jinguo Chen, Feng Gao, Zeqiu Han, Charles B. Underhill, and Lurong Zhang. *Dept. of Biology, Xiamen University, Xiamen, China, and Lombardi Cancer Ctr., Washington, DC.*

In previous studies, we have found that human brain hyaluronan binding protein (b-HABP) inhibits tumor growth. To explore the functional domain of this anti-tumor protein, 33 amino acids containing three hyaluronan binding motifs from N-terminal of b-HABP were linked with NGR homing motif to better target tumor cells. The synthetic peptide exerted an inhibitory effect on the proliferation of both TSU prostate cancer cells and HUVEC endothelial cells at a dose of 100 ug/ml. It also inhibited the colony formation of TSU and MDA-435 cells. When the targeted b-HABP peptide was tropically administrated to TSU and MD-A435 cells on top of the chorioallantoic membranes (CAM) of 10 days chicken embryos, the tumor growth was greatly inhibited. In addition, when 100 ug of b-HABP peptide was i.v. injected once into CAM bearing with established B16 melanomas, the growth of tumor xenografts was greatly inhibited. Then, the peptide sequence was back-translated into nucleotide sequence. The cDNA coding for the peptide was obtained using overlap-PCR and inserted into the pSecTag2 vector with a signal peptide for the secretion. The pSecTag2 vector alone (as control) or pSecTag2-peptide vectors (as tests) were transfected into MDA-435 cells. The in vivo results indicated that cells expressing targeted b-HABP peptide formed smaller tumors as compared to vector alone in both the CAM and nude mice model systems. Additional studies indicated that the targeted b-HABP peptide could damage the both the plasma membrane and mitochondrial membrane that triggered the apoptosis cascade.

#369 Anti-Tumor Effect of RGD-Tachyplesin. Yixin Chen, Xue-Ming Xu, Jinguo Chen, Ningfei Liu, Charles B. Underhill, Karen Creswell, Shuigen Hong, and Lurong Zhang. *Dept.of Biology, Xiamen University, Xiamen, China, and Lombardi Cancer Center, Washington, DC.*

Tachyplesin, an anti-microbial peptide present in leukocytes of horseshoe crab (Tachypleus tridentatus), was conjugated to the integrin homing domain RGD and tested for anti-tumor activity. Initial experiments indicated that RGD-tachyplesin could inhibit the proliferation of both cultured tumor and endothelial cells and could block the colony formation of TSU prostate cancer cells. The RGD-tachyplesin appeared to compromise the integrity of the plasma membrane as well as those associated with the mitochondria and nuclei, as evidenced by the changes in the staining with the fluorescent probes JC-1, annexin V, dextran-FITC and YO-PRO-1. In addition, Western blotting showed that the Fas ligand, FADD, Caspase 7, Caspase 6 and activated subunits of Caspase 8 (18 kDa) and Caspase 3 (20 kDa) were up-regulated following treatment with RGD-tachyplesin, suggesting that it induces apoptosis through elements of the Fas dependent pathway. And finally, in vivo studies indicated that the RGD-tachyplesin could inhibit the growth of tumor cells on the chorioallantoic membranes of chicken embryos and in syngenic mice. The results of this study suggests that the RGD-tachyplesin can inhibit tumor growth by impairing the function of vital membranes and by inducing apoptosis in both tumor cells and endothelial cells.

#4375 Human Brain Hyaluronan Binding Protein Inhibits Tumor Growth VIA Induction of Apoptosis.

Feng Gao, Xue-Ming Xu, Charles B. Underhill, Shimin Zhang, Ningfei Liu, Zeqiu Han, Jiaying Zhang, and Lurong Zhang. Lombardi Cancer Ctr., Washington, DC.

Naturally existing anti-tumor substance are less toxic and implicated a promising feature in cancer therapy. In this study, a new protein, termed human brain hyaluronan (HA) binding protein (b-HABP) was found to have an anti-tumor effect. The cDNA coding for N-terminal of human b-HABP was cloned and found to consist of 1,548 bp coding for 516 amino acids with signal peptide. When malignant MDA-435 breast cancer cells were transfected with b-HABP-pcDNA3, their ability to grow in anchorage-dependent conditions and to form colonies was greatly reduced compared to the mock transfectants. In addition, the conditioned media from b-HABP-pcDNA3 transfectants inhibited the growth of endothelial cells. Furthermore, studies revealed that the FasL, Caspase 3, p53, p27 were induced while bcl2 and cyclin E were reduced in b-HABP-pcDNA3 transfectants. Finally, the growth of tumors formed by b-HABP-pcDNA3 transfectants was greatly inhibited compared to the mock transfectants in CAM system and in nude mice model. This study suggests that HABP may represent a new category of naturally existing anti-tumor substance via induction of apoptosis.

#3465 Inhibition of Tumor Growth by Hyaluronan Binding Motifs (P4) is Mediated by Apoptosis Pathway Related with Lysosome and Mitochondria.

Ningfei Liu, Xue-Ming Xu, Charles Underhill, Susette Mueller, Karen Creswell, Yixin Chen, Jinguo Chen, and Lurong Zhang. Lombardi Cancer Ctr., Washington, DC.

We have demonstrated that the tumor growth can be greatly suppressed by hyaluronan binding motifs (P4) either exogenous administration of synthetic P4 peptide or endogenous expressing of P4. To explore the underlying mechanism for the anti-tumor effect, FITC-P4 was used for its intracellular tracing and the alterations in apoptotic molecules were studied. The results of confocal microscopy indicated that the P4 bound to cell surface, which could be partially blocked by anti-CD44, heparin and chondroitin sulfate, indicating that the binding may indirectly mediated by CD44 and interaction anionic substances on the membrane. Following the binding on cell surface, the FITC-P4 was up-taken by lysosomes and partially entered mitochondria, as evidenced by co-localization staining. At the molecular level, Fas ligand, FADD, caspase 8 (activated 18 kDa subunit) and caspase 3 were up-regulated upon the treatment of P4 in both MDA-435 tumor cells and ABAE endothelial cells, indicating that the apoptosis is triggered by P4. As a result, other vital membranes were greatly damaged as demonstrated by 1) positive Annexin V staining, an increased inflow of FITC-Dextran (MW 40,000) and exflow of LDH for the damage of plasma membrane; 2) an increased inflow of YO-Pro-1 for the damage of nuclear membrane; and 3) the shifted JC-1 staining for the depolarization of mitochondrial potential. Furthermore, the P4-induced cell death could be partially reversed by inhibitors (NH4Cl) specific for lysosomal functions and inhibitor (Z-VAD-FMK) for caspases, suggesting that the pro-apoptotic molecules associated with lysosome and mitochondria might be released by P4 and then activate the caspases in cytoplasm.

#4358 Effect of Tachyplesin on MDR Overexpressing Tumor Cells.

Jinguo Chen, Yixin Chen, Shuigen Hong, Fabio Leonessa, Robert Clarke, Xue-Ming Xu, Ningfei Liu, Charles B. Underhill, Karen Creswell, and Lurong Zhang. Lombardi Cancer Center, Georgetown University, Washington, DC, and The Key Lab of China Education Ministry on Cell Biology and Tumor Engineering, Xiamen University, Xiamen, China.

Tachyplesin is an anti-microbial peptide, consisting of 17 amino acids with a molecular weight of 2,269 Dalton and pI of 9.93. It has two disulfide linkages, which exposes all six positively charged basic amino acids on its surface. This cationic peptide can interact with anionic phospholipids present in the prokaryotic cytoplasmic membrane and eukaryotic mitochondrial membrane. We have found that tachyplesin could inhibit the growth of tumor cells. To see the effect of tachyplesin on the tumor cells that are resistant to first line chemotherapeutic drugs, we used a pair of breast cancer cell lines, LCC6-MDR (a MDA435 cells transduced with MDR1-retroviral vector) and LCC6-vector as control. Due to the over-expression of MDR1, LCC6-MDR cells resisted to Taxol with an EC50 of 1000 nM, while LCC6-vector had an EC50 of 10 nM. However, when treated with tachyplesin, both cell lines showed a similar sensitivity (EC50 of 40 nM) in response to the inhibitory effect of tachyplesin. The confocal analysis indicated that the FITC- tachyplesin bound to cell surface, entered the cells and localized in mitochondria. The flow cytometer analysis indicated that the mitochondria potential was depolarized and that both plasma membrane and nuclei membrane were damaged, as evidenced by staining with JC-1, FITC-Dextran and YO-Pro-1. This study suggests that the cationic peptide, such as tachyplesin, may be a promising alternative agent to treat the chemotherapy resistant tumor cells.